C^1 virtual element methods on polygonal meshes with curved edges

L. Beirão da Veiga,* D. Mora,† A. Silgado‡

Abstract

In this work we design a novel C^1-conforming virtual element method of arbitrary order $k \geq 2$, to solve the biharmonic problem on a domain with curved boundary and internal curved interfaces in two dimensions. By introducing a suitable stabilizing form, we develop a rigorous interpolation, stability, and convergence analysis obtaining optimal error estimates in the energy norm. Finally, we validate the theoretical findings through numerical experiments.

1 Introduction

Partial Differential Equations (PDEs) are fundamental in modeling several physical phenomena, such as fluid and solid mechanics, electromagnetic fields, heat conduction, among others. Although numerical schemes have significantly improved the ability to approximate the solution of PDEs, the complexity and challenge increase notably when these equations are posed on domains whose boundary is curved (or have internal curved interfaces). Such kinds of domains appear commonly in practical applications, including aerodynamics, biomedicine, geophysics, among others, where the geometries of interest do not conform to simple flat shapes. It is well known that standard numerical schemes that utilize meshes with straight edges approximate the curved interface/boundary of interest through a linear interpolation. This process introduces a geometry approximation error, which can significantly affect the analysis and the optimal rate of convergence, especially for schemes of higher-order (see for instance [47]). In order to overcome this drawback, several alternatives have been developed. For instance, among these we can find the isoparametric finite element [27, 49, 39], where high-order polynomial approximations of the curvilinear boundary is required, together with a careful choice of the isoparametric nodes. Another interesting approach is the isogeometric analysis [38, 9, 28], which can obtain the exact representation of computational (CAD) domains.

Recently, the curved virtual element method [15] has been presented as an alternative to avoid both the inconveniences associated with the effect of geometric error and the approach of finite isoparametric methods mentioned above. The Virtual Element Method (abbreviate, VEM) is a recent technology introduced in the pioneering work [10] (we also refer to [12] for some computational implementation aspects) and belongs to the group of polytopal Galerkin methods for discretizing PDEs. These schemes have garnered significant attention in recent years from the scientific community due to their inherent versatility in handling complex geometries. In particular, since its introduction, the VEM has been employed to discretize a wide range of problems in continuous mechanics. We refer to [5, 13] for a current state of the art on VEM and different applications.

It is well known that to construct conforming numerical schemes for fourth-order problems (in primal form) is required that the discrete spaces have C^1-continuity, this fact renders the methods highly complex. In particular, for the two-dimensional case, by employing traditional finite element schemes, polynomials of high-order are required to create C^1-approximations (e.g. degree fourth and five for the Bell and Argyris triangles, respectively), increasing the number of degrees of freedom and hence the computational complexity; for further details, we refer to [26, Chap. 6, sect. 6.1]. In contrast, the authors in [21] (see also [6, 25]), have been exploiting the ability of the VEM to construct discrete spaces with high-regularity. In particular, they have developed C^1-conforming

---

*Dipartimento di Matematica e Applicazioni, Università degli Studi di Milano Bicocca, Via Roberto Cozzi 55, Milano, Italy and IMATI-CNR, Via Ferrata 1, Pavia, Italy. E-mail: `lourenco.beirao@unimib.it`.

†GIMNAP, Departamento de Matemática, Universidad del Bío-Bío, Concepción, Chile and CI²MA, Universidad de Concepción, Concepción, Chile. E-mail: `dmora@ubiobio.cl`.

‡GIMNAP, Departamento de Matemática, Universidad del Bío-Bío, Concepción, Chile. E-mail: `asilgado@ubiobio.cl`.

schemes based on the VEM for solving fourth-order problems by employing low-order polynomials and few degrees of freedom; it can be seen that the lowest polynomial degree is $k = 2$, and the associated degrees of freedom are 3 per element vertex (the function and its gradient values vertex). In addition, we mention that VEM has also been applied to general polyharmonic problems, see for instance [7].

The applicability of the VEM to solve elliptic problems on domains with curves edges and internal interfaces in two dimensions was started in [15]. More precisely, the authors have been developed C^0-VEMs of high-order to solve the Poisson problem. By exploiting the facts that the VEM does not need an explicit expression of the basis functions and that the spaces are defined directly in physical domain (without using reference elements), the curvilinear approach enables the definition of discrete spaces within curved elements (directly), allowing an exact representation of the domain of interest by relying solely on a careful selection of the degrees of freedom and using a piecewise regular parametrization of the domain interface/boundary.

Since its introduction the approach of curved VEM has been employed to discretize several problems. For instance, in [8, 3] have been developed curvilinear virtual elements with application to two dimensional solid mechanics and contact problems. In [29, 31], the curved VEM in mixed formulations have been developed in two and three dimensions. The approach also has been utilized for approximating solutions to the wave equation [30]. Other approaches have been investigated in [36, 11, 17] for two and three dimensions.

On the other hand, in [16] the authors have been designed a curved VEM by employing the nonconforming approach, which is based on the computation of a novel Ritz-Galerkin operator that is different from the standard H^1-projection typically used in the VEM framework.

Further, different polytopic schemes have been developed to address curved domains. Among these, we mention the hybrid high-order method for the Poisson [18, 48] and the singularly perturbed fourth-order problems [32]; the unfitted hybrid high-order method [22]; then the extended hybridizable discontinuous Galerkin method [37] and the Trefftz-based finite element method [4].

In this work we are interested in solving the Biharmonic problem on domains with curved boundary by employing the approach presented in [15]. Fourth-order problems arise in many physical phenomena, for instance, in plate bending problems, fluid flow problems (in stream function form), the Cahn–Hilliard phase-field model, micro-electromechanical systems, among others. Due to its importance and challenging nature, several approaches have been devoted to the design of numerical schemes to solve these problems; see for instance [26, 23, 43, 33, 19], where classical conforming/nonconforming finite element schemes and C^0-IP methods have been developed. Additionally, several schemes and analyses addressing fourth-order problems by employing the C^1-conforming VE approach have been presented; see for instance [21, 25, 6, 41, 42, 35].

This paper is devoted to the design of C^1-conforming VEM of arbitrary order $k \geq 2$ on curved domains and the development of a rigorous interpolation, stability and convergence analysis, showing *optimal* error estimates in the H^2-norm. In particular, the proposed approach generalizes the C^1-VE space to the case of curved boundaries and internal interfaces. When the curved boundary is actually straight, the VE space and degrees of freedom of the proposed method simplifies to the space and degrees of freedom described in [21]. However, the definition of the stabilizing form remains different.

The construction of the present scheme is based on the approach developed in [15] for the simpler C^0-VEM for the Poisson equation. An adequate selection of the degrees of freedom and a piecewise regular parametrization of the domain boundary allow the construction of a computable H^2-VEM operator, and a computable load term in the virtual space. A rigorous interpolation, stability and convergence analysis is provided. It is interesting to note that such analysis cannot be accomplished by a standard extension of the arguments in [15]; the proving strategy of many important aspects needs to deviate considerably from the path laid in the mentioned article. This difficulty is related to the H^2 conformity required for the discrete space and the need to handle the associated higher-order terms on curved edges. Another peculiar challenge of the present approach is related to the preservation of the kernel of the involved bilinear form which for the simpler second-order diffusion problem is guaranteed by construction (since the local kernel is given by constant functions), while here it fails to be valid. Indeed, in the present approach, the space $V_k^h(E)$ does not contain the kernel of $a_E(\cdot, \cdot)$, i.e., $\mathbb{P}_1(E) \not\subset V_k^h(E)$ (see remarks 2.3 and 2.2). As a consequence, in order to prove stability and convergence of the scheme, we need to introduce a new stabilizing form, which is made of partial contributions of the degrees of freedom (the internals ones and the evaluations of the function and its gradient at the vertexes), plus integrals on edges involving tangential and normal derivatives of the virtual functions (see below (2.9) and (2.10)). This change is motivated by the fact that, the classical choice for the stabilizing form, i.e., the "*dofi-dofi*" stabilization [10, 21], is not guaranteed to satisfy the coercivity property in the space $V_k^h(E) + \mathbb{P}_1(E)$.

Finally, in the last section of the article we present a set of numerical tests underlining the optimal behaviour of the scheme also from the practical perspective.

Preliminary notations and model problem. For any open bounded Lipschitz domain $\mathcal{D}$ in $\mathbb{R}^2$, and for $t \geq 0$, we will employ the usual notation for the Sobolev spaces $H^t(\mathcal{D})$, according to Reference [1], with their corresponding seminorm and norms denoted by $|\cdot|_{t,\mathcal{D}}$ and $\|\cdot\|_{t,\mathcal{D}}$, respectively. In the particular case $t = 0$, we write $L^2(\mathcal{D})$ instead of $H^0(\mathcal{D})$ and its standards L^2 inner-product and norm are denote by $(\cdot, \cdot)_{0,\mathcal{D}}$ and $\|\cdot\|_{0,\mathcal{D}}$. Furthermore, we introduce the Sobolev spaces $W^{s,\infty}(\mathcal{D})$, $s \in \mathbb{N} \cup \{0\}$, of functions having weak derivatives up to order s, which are bounded almost everywhere in $\mathcal{D}$. The particular case $s = 0$ coincides with the space $L^\infty(\mathcal{D})$. As usual, the spaces of non-integer order $s > 0$, are constructed by interpolation theory. The corresponding seminorm and norm are denote by $|\cdot|_{W^{s,\infty}(\mathcal{D})}$ and $\|\cdot\|_{W^{s,\infty}(\mathcal{D})}$, respectively. Moreover, with the usual notation the symbols ∇v, Δv, $\Delta^2 v$ and $\mathbf{D}^2 v$ denote the gradient, the Laplacian, the Bilaplacian and the Hessian matrix for a regular enough scalar function v.

From now on, Ω will denote a Lipschitz domain in $\mathbb{R}^2$ with (possibly) curved boundary $\Gamma := \partial\Omega$ and unit outward normal $\mathbf{n}$. We consider the Biharmonic problem with homogeneous Dirichlet boundary conditions, which reads as: given $f \in L^2(\Omega)$, find $u : \Omega \to \mathbb{R}$ such that

$$\begin{cases} \Delta^2 u = f & \text{in } \Omega, \\ u = \partial_{\mathbf{n}} u = 0 & \text{on } \Gamma. \end{cases} \tag{1.1}$$

A variational formulation of problem (1.1) reads as follows: find $u \in V := H_0^2(\Omega)$, such that

$$a(u, v) = (f, v)_{0,\Omega} \qquad \forall v \in V, \tag{1.2}$$

where the bilinear form is given by:

$$a(u, v) := (\mathbf{D}^2 u, \mathbf{D}^2 v)_{0,\Omega} \qquad \forall u, v \in V. \tag{1.3}$$

By using that $\|\mathbf{D}^2 \cdot \|_{0,\Omega}$ is a norm equivalent to the H^2-norm, we have that the bilinear form $a(\cdot, \cdot)$ is V-elliptic. Thus, problem (1.2) is well posed as a consequence of the Lax-Milgram Theorem.

Now, we will consider additional notations and settings. For the domain Ω, we assume that its boundary Γ is the union a finite number of smooth curves $\{\Gamma_i\}_{i=1}^N$, i.e.,

$$\Gamma = \bigcup_{i=1}^N \Gamma_i.$$

Moreover, we consider the following assumption:

(A0) the boundary Γ is Lipschitz and each curve Γ_i of Γ is sufficiently smooth, namely we require that Γ_i is of class $C^{\alpha+1}$, with $\alpha \geq 0$ to be better specified later.

Let $I_i := [a_i, b_i] \subset \mathbb{R}$ be a closed interval of $\mathbb{R}$ and $\gamma_i : I_i \to \Gamma_i$ be a given regular and invertible $C^{\alpha+1}$-parametrization of the curve Γ_i, for $i = 1, \ldots, N$.

In what follows, as all parts Γ_i of $\partial\Omega$ will be handled similarly, for the sake of simplicity in notation, we will omit the index i from the related maps and parameters.

Outline. The layout of this paper is as follows. In Section 2 we first introduce some notations and basic settings on the regular polygonal meshes, and afterwards describe the virtual element spaces together with their degrees of freedom, the discrete forms and the VE formulation. In Section 3, we provide a rigorous analysis for the proposed VE scheme. In particular, we establish interpolation, stability and convergence analysis for the method. In Section 4, we report some numerical experiments that corroborate the theoretical results obtained in the previous section.

2 The C^1 virtual element scheme on curved domains

In this section we introduce a family of C^1-conforming VEMs for the numerical approximation of problem (1.2) of arbitrary order $k \geq 2$ on curved domains. First, we introduce some ingredients to construct the discrete virtual scheme, such as, notations on the polygonal decompositions, local and global virtual spaces together with their corresponding degrees of freedom, polynomial projections, the discrete bilinear forms and the load term approximation. We conclude this section presenting the discrete VE formulation.

2.1 Notations and basic settings on the polygonal decompositions

Mesh assumptions. Henceforth, we will denote by E a general polygon, and by e a general edge of ∂E (possibly curved). We denote by h_E the diameter of the element E and by h_e the size of the edge e, where the size of an edge is the distance between its two endpoints (see below Remark 2.1). Moreover, we will denote by x_e and $\mathbf{x}_E$ the midpoint of e and the baricenter of E, respectively. For each element E, we denote by N_E the number of vertices of E, by N_e the number of edges of E. We associate the outward unit normal vector $\mathbf{n}_E$ and the unit tangent vector $\mathbf{t}_E$ to E. Although for a polygon the quantities N_E and N_e are the same, we prefer to denote them differently.

Let $\{\Omega_h\}_{h>0}$ be a sequence of decompositions of Ω into general non-overlapping polygons E, where $h := \max_{E \in \Omega_h} h_E$. For all h, we will consider the classical regularity assumptions on the decomposition Ω_h: there exist a positive constant ρ independent of h, such that

(A1) E is star-shaped with respect to a ball B_E of radius $\geq \rho\, h_E$,

(A2) the length of any (possibly curved) edge of E is $\geq \rho\, h_E$,

We will write $a \lesssim b$ and $a \gtrsim b$ instead of $a \leq Cb$ and $a \geq Cb$, respectively, where C is positive constant independent of the decomposition Ω_h. Further, we write $a \approx b$ when $a \lesssim b$ and $b \lesssim a$ occur at the same time. The involved constants will be explicitly written only when necessary.

Assumptions **(A1)**–**(A2)** imply that each element E has a uniformly bounded number of edges. Moreover, it guarantees that the constants in the forthcoming trace and inverse inequalities are uniformly bounded.

Remark 2.1 *Let $L_e = \int_{I_e} \|\gamma'(t)\|$ be the length of a curved edge. Since γ and γ^{-1} are fixed once and for all, and both are of class $W^{1,\infty}$, we have that the values h_e and L_e are comparable. Therefore in what follows, by simplicity we will refer to both quantities as "length" of e.*

Related polynomial spaces. Let $\mathbb{P}_\ell(E)$, $\ell \in \mathbb{N}$, be the space of polynomials of maximum degree ℓ over each element E, with the convention $\mathbb{P}_{-2}(E) = \mathbb{P}_{-1}(E) = \{0\}$. We introduce a basis for the space $\mathbb{P}_\ell(E)$ given by the set of shifted and scaled monomials:

$$\mathbb{M}_\ell(E) = \left\{ \left(\frac{\mathbf{x} - \mathbf{x}_E}{h_E} \right)^{\boldsymbol{\alpha}} \forall \boldsymbol{\alpha} \in \mathbb{N}^2,\ |\alpha| \leq \ell,\ \forall \mathbf{x} \in E \right\},$$

where $\boldsymbol{\alpha}$ denotes a multi-index $\boldsymbol{\alpha} = (\alpha_1, \alpha_2)$.

Similarly, we consider the space of polynomials of maximum degree ℓ over the interval I_e, which is defined by $\mathbb{P}_\ell(I_e)$, with $\ell \in \mathbb{N}$. Given x_{I_e} and h_{I_e} the midpoint and the length of I_e, we introduce a basis for the polynomial space $\mathbb{P}_\ell(I_e)$ given by the following set of shifted and scaled monomials:

$$\mathbb{M}_\ell(I_e) = \left\{ \left(\frac{x - x_{I_e}}{h_{I_e}} \right)^{\alpha} \forall \alpha \in \mathbb{N},\ \alpha \leq \ell,\ \forall x \in I_e \right\}.$$

Since $\gamma_e : I_e \to e$ denotes the parametrization of the edge e, we consider the following mapped polynomial space:

$$\widetilde{\mathbb{P}}_\ell(e) = \left\{ \widetilde{q_\ell} = \widehat{q_\ell} \circ \gamma_e^{-1} :\ \widehat{q_\ell} \in \mathbb{P}_\ell(I_e) \right\}. \tag{2.1}$$

Clearly, whenever e is straight (in which case we always take γ as an affine mapping), the space $\widetilde{\mathbb{P}}_\ell(e)$ correspond to the standard polynomial space $\mathbb{P}_\ell(e)$.

Finally, we define the piecewise ℓ-order polynomial space by:

$$\mathbb{P}_\ell(\Omega_h) := \{ q \in L^2(\Omega) : q|_E \in \mathbb{P}_\ell(E) \quad \forall E \in \Omega_h \}.$$

2.2 Virtual element spaces and their degrees of freedom

In this subsection we introduce a family of conforming virtual element spaces on curved domains and endow such spaces with suitable sets of degrees of freedom. For simplicity of exposition, in the following we will assume that every element E has at most one curved edge lying on Γ (hence, only one edge of E will be curved and the remaining will be straight); the extension to the case with more curved edges is trivial. Moreover, we assume that

each curved edge lies on only one regular curve, i.e, $e \subseteq \Gamma_i$. This last condition is mandatory for the approach followed in this work.

In the following we assume to have integration rules which allow the accurate integration of smooth functions on curved polygons and on curved edges; these indeed exist in the literature, see for instance [45, 46, 24].

Let $E \in \Omega_h$ with $\partial E = \bigcup_{i=1}^{N_E} e_i$, where $e_1 \subset \Gamma$, and $e_2, \cdots, e_{N_E}$ are straight segments. Thus, for each integer $k \geq 2$ we introduce the index $r := \max\{k, 3\}$ and the local virtual space on the curved element E:

$$V_k^h(E) := \Big\{ v_h \in H^2(E) \cap C^1(\partial E) : \Delta^2 v_h \in \mathbb{P}_{k-4}(E), \ v_h|_{e_1} \in \widetilde{\mathbb{P}}_r(e_1), \ \partial_{\mathbf{n}_E} v_h|_{e_1} \in \widetilde{\mathbb{P}}_{k-1}(e_1),$$

$$v_h|_{e_i} \in \mathbb{P}_r(e_i), \ \partial_{\mathbf{n}_E} v_h|_{e_i} \in \mathbb{P}_{k-1}(e_i) \quad \text{for } i = 2, \ldots, N_E \Big\}. \quad (2.2)$$

Remark 2.2 *From definition* (2.2) *it is clear that if the polygon E has at least a curved edge, then $\mathbb{P}_0(E) \subseteq V_k^h(E)$ but $\mathbb{P}_k(E) \not\subset V_k^h(E)$. The property $\mathbb{P}_0(E) \subseteq V_k^h(E)$ was critical in the analysis of [15] since $\mathbb{P}_0(E)$ represents the local kernel for the simpler Poisson equation. Here, the local kernel of the involved bilinear form is $\mathbb{P}_1(E)$, which is not contained in $V_k^h(E)$. Therefore, we need to be more careful in constructing the discrete approximated bilinear form $a^h(\cdot, \cdot)$, especially with the design of the stabilizing part $\mathcal{S}_E(\cdot, \cdot)$; see below* (2.9).

For each $v_h \in V_k^h(E)$, we define the following sets of linear functionals $\boldsymbol{D}$ (split into boundary operators $\boldsymbol{D}^\partial$ and internal ones $\boldsymbol{D}^o$):

- $\boldsymbol{D}_I^\partial$: the values of v_h at the vertexes $\mathbf{v}_i$ for $i = 1, \ldots, N_E$ of the element E;

- $\boldsymbol{D}_{II}^\partial$: the values of $h_{\mathbf{v}_i} \nabla v_h$ at the vertexes $\mathbf{v}_i$ for $i = 1, \ldots, N_E$ of the element E;

- $\boldsymbol{D}_{III}^\partial$: the values of v_h at $k_e = \max\{0, k-3\}$ internal points of the $(k+1)$-point Gauss-Lobatto quadrature rule of every straight edge $e_2, \ldots, e_{N_E} \in \partial E$;

- $\boldsymbol{D}_{IV}^\partial$: the values of v_h at $k_e = \max\{0, k-3\}$ internal points of e_1 that are the images through γ of the k_e internal points of the $(k+1)$-point Gauss-Lobatto quadrature on I_{e_1};

- $\boldsymbol{D}_V^\partial$: the values of $h_e \partial_{\mathbf{n}_E} v_h$ at $k_{\mathbf{n}} = k-2$ internal points of the k-point Gauss-Lobatto quadrature rule of every straight edge $e_2, \ldots, e_{N_E} \in \partial E$;

- $\boldsymbol{D}_{VI}^\partial$: the values of $h_e \partial_{\mathbf{n}_E} v_h$ at $k_{\mathbf{n}} = k-2$ internal points of e_1 that are the images through γ of the $k_{\mathbf{n}}$ internal points of the k-point Gauss-Lobatto quadrature on I_{e_1},

- $\boldsymbol{D}^o$: for $k \geq 4$, the internal moments of v_h against the scaled monomials $\{m_j\}_{j=1}^{(k-3)(k-2)/2} \in \mathbb{M}_{k-4}(E)$, i.e.,

$$\boldsymbol{D}_j^o(v_h) := h_E^{-2} \int_E v_h \, m_j \, \mathrm{d}E,$$

where $h_{\mathbf{v}_i}$ corresponds to the average of the diameters corresponding to the elements with $\mathbf{v}_i$ as a vertex. A visualization of these DoFs on a curved pentagon can be seen in Figure 1, for the cases $k = 3$ and $k = 4$.
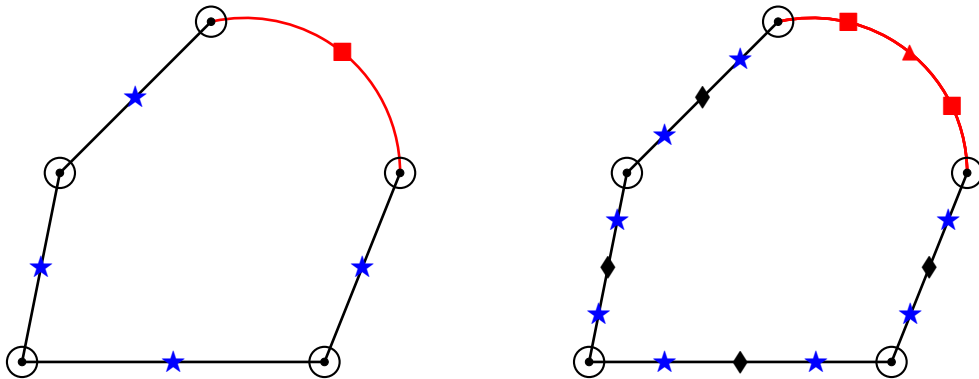

Figure 1: DoFs for $k = 3$ (left) and $k = 4$ (right). We denote $\boldsymbol{D}_I^\partial$ with the dots, $\boldsymbol{D}_{II}^\partial$ with the circles, $\boldsymbol{D}_{III}^\partial$ with the black diamonds, $\boldsymbol{D}_{IV}^\partial$ with the red triangles, $\boldsymbol{D}_V^\partial$ with the blue stars, and $\boldsymbol{D}_{VI}^\partial$ with the red squares.

For all $E \in \Omega_h$, we have that the dimension of the local space $V_k^h(E)$ is

$$\dim(V_k^h(E)) = (3 + k_e + k_\mathbf{n})N_e + \frac{(k-3)(k-2)}{2}. \tag{2.3}$$

The following result generalizes [21, Proposition 4.2] to the case of polygons with curved edges. Although the proof is quite predictable, we prefer to report it in detail for completeness.

Theorem 2.1 *The sets of linear functionals $\mathbf{D}$ are a set of degrees of freedom for the space $V_k^h(E)$.*

Proof. We observe that the cardinal of sets $\mathbf{D}$ is equal to the dimension of the space $V_k^h(E)$ (cf. (2.2) and (2.3)), therefore it is sufficient to show that any virtual function with vanishing DoFs is the zero function. Using integration by parts, we have

$$\int_E |\Delta v_h|^2 \mathrm{d}E = \int_E v_h \Delta^2 v_h \mathrm{d}E + \int_{\partial E} \partial_{\mathbf{n}_E} v_h \Delta v_h \mathrm{d}s - \int_{\partial E} v_h \partial_{\mathbf{n}_E} \Delta v_h \mathrm{d}s.$$

Following standard VEM arguments, the key point becomes to prove that $\mathbf{D}_{\mathbf{i}}^{\partial}(v_h) = \mathbf{0}$, with $\mathbf{i} \in \{\mathbf{I}, \mathbf{II}, \mathbf{IV}, \mathbf{VI}\}$ imply that $v_h|_{e_1} \equiv 0$ and $\partial_{\mathbf{n}_E} v_h|_{e_1} \equiv 0$ (since for the straight edges and the volume part the proof is standard). We first analyze the cases $k = 2$ and $k = 3$.

For the case $k = 2$, we have $r = \max\{3, k\} = 3$. Thus, $v_h|_{e_1} \in \widetilde{\mathbb{P}}_3(e_1)$ and $\partial_{\mathbf{n}_E} v_h|_{e_1} \in \widetilde{\mathbb{P}}_1(e_1)$. We denote by $\mathbf{v}_{e_1}^{\mathrm{i}}$ and $\mathbf{v}_{e_1}^{\mathrm{f}}$ the initial and end points of e_1, respectively. Then, from the definition of normal derivative and $\mathbf{D}_{\mathbf{II}}^{\partial}$ we have

$$\partial_{\mathbf{n}_E} v_h(\mathbf{v}_{e_1}^{\mathrm{i}}) = \partial_{\mathbf{n}_E} v_h(\mathbf{v}_{e_1}^{\mathrm{f}}) = 0,$$

thus $\partial_{\mathbf{n}_E} v_h|_{e_1} \equiv 0$. Now, since $v_h|_{e_1} \in \widetilde{\mathbb{P}}_3(e_1)$, from definition of (2.1), we have

$$v_h(\gamma(t)) = \widetilde{q_3}(\gamma(t)) = \widehat{q_3}(t) \qquad \forall t \in I_{e_1},$$

where $\widehat{q_3} \in \mathbb{P}_3(I_{e_1})$. Then, by applying the chain rule to functions of two variables, we obtain

$$\frac{d\widehat{q_3}(t)}{dt} = \nabla v_h(\gamma(t)) \cdot \frac{d\gamma(t)}{dt},$$

where ∇v_h is the gradient of v_h and $\frac{d\gamma(t)}{dt}$ denotes the derivatives vector respect with the parameter t of the γ-components.

Now, let $\{H_1, H_2, H_3, H_4\}$ be the four polynomials of the Hermite basis, then by employing the above facts, we get

$$\begin{aligned}
\widehat{q_3}(t) &= \widehat{q_3}(a_1)H_1(t) + \frac{d\widehat{q_3}(a_1)}{dt}H_2(t) + \widehat{q_3}(b_1)H_3(t) + \frac{\widehat{q_3}(b_1)}{dt}H_4(t) \\
&= v_h(\gamma(a_1))H_1(t) + \nabla v_h(\gamma(a_1)) \cdot \frac{d\gamma(a_1)}{dt}H_2(t) + v_h(\gamma(b_1))H_3(t) + \nabla v_h(\gamma(b_1)) \cdot \frac{d\gamma(b_1)}{dt}H_4(t) \\
&= v_h(\gamma(a_1))H_1(t) + \nabla v_h(\mathbf{v}_{e_1}^{\mathrm{i}}) \cdot \frac{d\gamma(a_1)}{dt}H_2(t) + v_h(\gamma(b_1))H_3(t) + \nabla v_h(\mathbf{v}_{e_1}^{\mathrm{f}}) \cdot \frac{d\gamma(b_1)}{dt}H_4(t),
\end{aligned}$$

where we have used that $\gamma(a_1) = \mathbf{v}_{e_1}^{\mathrm{i}}$ and $\gamma(b_1) = \mathbf{v}_{e_1}^{\mathrm{f}}$. Therefore, by employing that $\mathbf{D}_{\mathbf{I}}^{\partial}(v_h) = \mathbf{D}_{\mathbf{II}}^{\partial}(v_h) = \mathbf{0}$, it implies $\widehat{q_3} = 0$, and thus $v_h|_{e_1} \equiv 0$.

For the case $k = 3$, we have $v_h|_{e_1} \in \widetilde{\mathbb{P}}_3(e_1)$ and $\partial_{\mathbf{n}_E} v_h|_{e_1} \in \widetilde{\mathbb{P}}_2(e_1)$. Now, let $\{t_j\}_{j=1}^3$ represent the nodes of the 3-point Gauss-Lobatto quadrature on I_{e_1}. Then, by using the definition (2.1) and $\mathbf{D}_{\mathbf{VI}}^{\partial}(v_h) = 0$, we have

$$0 = \partial_{\mathbf{n}_E} v_h(\gamma(t_2)) = \widetilde{q_2}(\gamma(t_2)) = \widehat{q_2}(t_2),$$

where $\widehat{q_2} \in \mathbb{P}_2(I_{e_1})$. Moreover, as in the case $k = 2$, we have $\partial_{\mathbf{n}_E} v_h(\mathbf{v}_{e_1}^{\mathrm{i}}) = \partial_{\mathbf{n}_E} v_h(\mathbf{v}_{e_1}^{\mathrm{f}}) = 0$, and using $\gamma(a_1) = \mathbf{v}_{e_1}^{\mathrm{i}}$, $\gamma(b_1) = \mathbf{v}_{e_1}^{\mathrm{f}}$, we conclude $\widehat{q_2}(t_i) = 0$, for $i = 1, 2, 3$. Therefore $\widehat{q_2} \equiv 0$, that implies $\partial_{\mathbf{n}_E} v_h|_{e_1} \equiv 0$. The fact $v_h|_{e_1} \equiv 0$ follows exactly as in case $k = 2$.

So far we have shown $v_h|_{e_1} \equiv 0$ and $\partial_{\mathbf{n}_E} v_h|_{e_1} \equiv 0$ for $k = 2$ and $k = 3$. Now, we will consider the case $k \geq 4$. In this case, we have $r = k$, so $v_h|_{e_1} \in \widetilde{\mathbb{P}}_k(e_1)$ and $\partial_{\mathbf{n}_E} v_h|_{e_1} \in \widetilde{\mathbb{P}}_{k-1}(e_1)$. By definition, there exists $\widehat{q_k} \in \mathbb{P}_k(I_{e_1})$, such that

$$v_h(\gamma(t)) = \widetilde{q_k}(\gamma(t)) = \widehat{q_k}(t) \qquad \forall t \in I_{e_1},$$

Let $\{f_1, f_2, \ldots, f_{n_k}\}$ be the canonical basis associated to the sets $\boldsymbol{D_I^\partial}, \boldsymbol{D_{II}^\partial}$ and $\boldsymbol{D_{IV}^\partial}$, where $n_k = \dim(\mathbb{P}_k(I_{e_1}))$, such that the canonical functions f_1, f_2, f_{n_k-1} and f_{n_k} are associated to the canonical coefficients $\widehat{q}_k(a_1), \frac{d\widehat{q}_k(a_1)}{dt}$, $\widehat{q}_k(b_1)$ and $\frac{d\widehat{q}_k(b_1)}{dt}$, respectively. Thus, as in the case $k = 2$, for all $t \in I_{e_1}$, from the chain rule we have

$$\widehat{q}_k(t) = \widehat{q}_k(a_1)f_1(t) + \frac{d\widehat{q}_k(a_1)}{dt}f_2(t) + \alpha_3 f_3(t) + \cdots + \alpha_{n_k-2}f_{n_k-2}(t) + \widehat{q}_k(b_1)f_{n_k-1}(t) + \frac{d\widehat{q}_k(b_1)}{dt}f_{n_k}(t)$$

$$= v_h(\gamma(a_1))f_1(t) + \nabla v_h(\gamma(a_1)) \cdot \frac{d\gamma(a_1)}{dt} + \alpha_3 f_3(t) + \cdots + \alpha_{n_k-2}f_{n_k-2}(t)$$

$$+ v_h(\gamma(b_1))f_{n_k-1}(t) + \nabla v_h(\gamma(b_1)) \cdot \frac{d\gamma(b_1)}{dt}f_{n_k}(t).$$

Thus, by using $\boldsymbol{D_I^\partial}(v_h) = \boldsymbol{D_{II}^\partial}(v_h) = \boldsymbol{D_{IV}^\partial}(0) = \mathbf{0}$, we obtain that $\widehat{q}_k \equiv 0$, hence $v_h|_{e_1} \equiv 0$. The fact $\partial_{\mathbf{n}} v_h|_{e_1} \equiv 0$ follows from the same arguments used in the case $k = 3$.

$\square$

The global virtual element space is constructed by combining of the local spaces $V_k^h(E)$ and incorporating the homogeneous Dirichlet boundary conditions, i.e., for every decomposition Ω_h into polygons E, we define

$$V_k^h = \{v_h \in V : v_h|_E \in V_k^h(E) \quad \forall E \in \Omega_h\}, \tag{2.4}$$

with the obvious associated sets of global degrees of freedom.

We notice that the unisolvency of global DoFs follows from the unisolvency of the local degrees of freedom and the definition of the local and global VE spaces.

2.3 Polynomial projectors and discrete forms

In this subsection we introduce some polynomial projections and the discrete bilinear form approximating the continuous form (1.3). Moreover, we propose an approximation for the load term.

As usual, we decompose into local contributions the bilinear form $a(\cdot, \cdot)$ defined in (1.3) as follows

$$a(u, v) = \sum_{E \in \Omega_h} a_E(u, v) \qquad \forall u, v \in V.$$

Polynomial projections. Next, we shall construct a VEM H^2-projection. Indeed, for each polygon E, we define the projector $\Pi_E^{\mathbf{D},k} : H^2(E) \to \mathbb{P}_k(E)$, as the solution of the local problems:

$$a_E(v_h - \Pi_E^{\mathbf{D},k}v_h, q_k) = 0 \qquad \forall q_k \in \mathbb{P}_k(E),$$
$$\Pi_{\partial E}^0(v_h - \Pi_E^{\mathbf{D},k}v_h) = 0, \quad \Pi_{\partial E}^0(\nabla(v_h - \Pi_E^{\mathbf{D},k}v_h)) = 0, \tag{2.5}$$

where the operator $\Pi_{\partial E}^0 : H^1(E) \to \mathbb{P}_0(E)$ is given by:

$$\Pi_{\partial E}^0\varphi := |\partial E|^{-1} \int_{\partial E} \varphi \, \mathrm{d}s. \tag{2.6}$$

Furthermore, for each $m \in \mathbb{N} \cup \{0\}$ we consider the usual L^2-projection $\Pi_E^m : L^2(E) \to \mathbb{P}_m(E)$, defined by

$$\int_E (v - \Pi_E^m v)p_m = 0 \qquad \forall p_m \in \mathbb{P}_m(E). \tag{2.7}$$

The following result is easy to check by standard VEM arguments (see for instance [21]).

Proposition 2.1 *For each $k \geq 2$ the operator $\Pi_E^{\mathbf{D},k} : H^2(E) \to \mathbb{P}_k(E)$ defined in (2.5) is computable from the degrees of freedom $\boldsymbol{D}$. Moreover, for $k \geq 4$ the L^2-projection Π_E^{k-4} defined in (2.7) is computable from the degrees of freedom $\boldsymbol{D^o}$.*

Discrete bilinear forms. The next step consists in constructing a computable approximation of the bilinear form (1.3) with the tools given above. Indeed, first we define the following local bilinear form. Recalling Remark 2.2, we consider the space

$$\mathbb{V}_k^h(E) := V_k^h(E) + \mathbb{P}_k(E). \tag{2.8}$$

Then, we set the following bilinear form

$$a_E^h \colon \mathbb{V}_k^h(E) \times \mathbb{V}_k^h(E) \to \mathbb{R},$$

approximating the local continuous form $a_E(\cdot,\cdot)$, and defined by

$$a_E^h(v_h, w_h) := a_E\big(\Pi_E^{\mathbf{D},k} v_h, \Pi_E^{\mathbf{D},k} w_h\big) + \mathcal{S}_E\big((I - \Pi_E^{\mathbf{D},k})v_h, (I - \Pi_E^{\mathbf{D},k})w_h\big) \qquad \forall v_h, w_h \in \mathbb{V}_k^h(E),$$

where the form $\mathcal{S}_E \colon \mathbb{V}_k^h(E) \times \mathbb{V}_k^h(E) \to \mathbb{R}$ is an adequate symmetric stabilizing bilinear form, which is computable by using the degrees of freedom $\boldsymbol{D}$.

In the present approach we need to introduce the following peculiar stabilizing form (see remarks 2.2 and 2.3):

$$\mathcal{S}_E(\eta_h, \sigma_h) := h_E^{-2} \sum_{j=1}^{(k-3)(k-2)/2} \boldsymbol{D}_j^{\circ}(\eta_h)\boldsymbol{D}_j^{\circ}(\sigma_h) + \sum_{i=1}^{3N_E} h_{\mathbf{v}_i}^{-2} \boldsymbol{D}_i^{\partial,\mathbf{v}}(\eta_h)\boldsymbol{D}_i^{\partial,\mathbf{v}}(\sigma_h)$$
$$+ h_E \sum_{i=1}^{N_e} \big((\partial_{\mathbf{t}_E}(\partial_{\mathbf{n}_E}\eta_h), \partial_{\mathbf{t}_E}(\partial_{\mathbf{n}_E}\sigma_h))_{0,e_i} + (\partial_{\mathbf{t}_E}^2 \eta_h, \partial_{\mathbf{t}_E}^2 \sigma_h)_{0,e_i}\big) \qquad \forall \eta_h, \sigma_h \in \mathbb{V}_k^h(E), \tag{2.9}$$

where $\boldsymbol{D}^{\partial,\mathbf{v}}$ is the vector of DoFs associated with the boundary DoFs $\boldsymbol{D}_I^{\partial}$ and $\boldsymbol{D}_{II}^{\partial}$.

We observe that this bilinear form can be rewritten as the sum of three terms: the first, $\mathcal{S}_E^{\circ}$, involving the internal DoFs, the second $\mathcal{S}_E^{\partial,\mathbf{v}}$ involving the vertex boundary DoFs, and the third $\mathcal{S}_E^{\partial,e}$ involving edges integrals as follows

$$\mathcal{S}_E(\eta_h, \sigma_h) = \mathcal{S}_E^{\circ}(\eta_h, \sigma_h) + \mathcal{S}_E^{\partial,\mathbf{v}}(\eta_h, \sigma_h) + \mathcal{S}_E^{\partial,e}(\eta_h, \sigma_h) \qquad \forall \eta_h, \sigma_h \in \mathbb{V}_k^h(E). \tag{2.10}$$

Finally we introduce the global bilinear form $a^h \colon \mathbb{V}_k^h \times \mathbb{V}_k^h \to \mathbb{R}$ given by

$$a^h(u_h, v_h) = \sum_{E \in \Omega_h} a_E^h(u_h, v_h) \qquad \forall u_h, v_h \in \mathbb{V}_k^h. \tag{2.11}$$

Remark 2.3 *The new stabilizing form $\mathcal{S}_E(\cdot,\cdot)$ defined in (2.9) is fully computable by using the DoFs $\boldsymbol{D}$. Furthermore, differently from more standard choices such as the "dofi-dofi" stabilization [10, 21], the form (2.9) satisfies the coercivity property also in the sum space $V_k^h(E) + \mathbb{P}_1(E)$ (see Lemma 3.8).*

Load term approximation. Here we shall define the discrete load term. As in [21], we will consider different approximations for the load term, depending on the polynomial degree k. Indeed, first we will introduce some useful notations

$$f_h|_E := \begin{cases} \Pi_E^{k-2} f & \text{if } k = 2, 3, \\ \Pi_E^1 f & \text{if } k = 4, \\ \Pi_E^{k-4} f & \text{if } k > 4, \end{cases}$$

$$\widehat{\Pi}_E^1 v_h := \begin{cases} \widehat{v_h} + (k-2)(\mathbf{x} - \mathbf{x}_E) \cdot \widehat{\nabla v_h} & \text{if } k = 2, 3, \\ \Pi_E^0 v_h + (\mathbf{x} - \mathbf{x}_E) \cdot \widehat{\nabla v_h} & \text{if } k = 4, \end{cases}$$

where

$$\widehat{w_h} = \frac{1}{N_E} \sum_{i=1}^{N_E} w_h(\mathbf{v}_i), \quad \text{with } \mathbf{v}_i, 1 \le i \le N_E \text{ are the vertices of } E.$$

Then, the right-hand side is defined by

$$\langle f_h, v_h \rangle := \begin{cases} \sum_{E \in \Omega_h} (f_h, \widehat{\Pi}_E^1 v_h)_{0,E} & \text{if } k = 2, 3, 4, \\ \sum_{E \in \Omega_h} (f_h, v_h)_{0,E} & \text{if } k > 4. \end{cases} \tag{2.12}$$

We observe that the right-hand side defined above is computable by using the DoFs $\boldsymbol{D}$.

Remark 2.4 *By combining the ideas in [2] with the advancements presented here, it is possible to design enhanced versions of the local spaces presented in (2.2), allowing to compute exactly also the higher-order projection $\Pi_E^{k-2} \colon V_k^h(E) \to \mathbb{P}_{k-2}(E)$, for $k \geq 2$. In this case, we can simply take $f_h|_E := \Pi_E^{k-2}$, for all $E \in \Omega_h$ in order to derive optimal estimates in L^2- and H^1-norms. We refer to [25, 6] for enhanced versions of the C^1-VEM with straight edges.*

The virtual element formulation. With the above definitions we are in a position to write the conforming discrete VE formulation. The VE problem reads as: find $u_h \in V_k^h$, such that

$$a^h(u_h, v_h) = \langle f_h, v_h \rangle \qquad \forall v_h \in V_k^h, \tag{2.13}$$

where the bilinear form $a^h(\cdot, \cdot)$ and discrete load term f_h are defined in (2.11) and (2.12), respectively.

The well-posedness of discrete problem (2.13) follows from the fact that, by construction, the bilinear form $a^h(\cdot, \cdot)$ is symmetric and coercive on the space V_k^h. This last fact will be rigorously investigated in Section 3.3.

We point out that if Ω is a domain with polygonal boundary Γ, i.e., if Γ is made up of a finite number of straight sides, and the stabilizing form $\mathcal{S}_E(\cdot, \cdot)$ is defined as the classical "*dofi-dofi*" stabilization, then we recover the C^1-VEM proposed in [21] apart for the choice of the stabilization.

Remark 2.5 *We again underline that the present approach (and analysis) is immediately applicable to the case of curved internal interfaces since the provided DoFs guarantee the global continuity of the discrete functions also across curved edges. Assuming curved edges only on the boundary Γ simplifies the exposition.*

3 Theoretical analysis

This section is devoted to the interpolation, stability and convergence analysis. For a regular enough function we will construct an interpolant in the virtual element space V_k^h and prove optimal approximation properties. Moreover, we present stability bounds for the stabilization (2.10). Finally, with the help of these previous properties, we provide the well-posedness and a priori error estimates for the proposed method.

3.1 Preliminary results

We start reviewing some preliminary results, which will be useful in the forthcoming section.

Lemma 3.1 *Let $k \in \mathbb{N}$. Then, for all $E \in \Omega_h$ and $v \in H^s(E)$, there exists a polynomial function $v_\pi \in \mathbb{P}_k(E)$, such that*

$$|v - v_\pi|_{r,E} \lesssim h_E^{s-r} |v - v_\pi|_{s,E} \lesssim h_E^{s-r} |v|_{s,E},$$

*for all $r, s \in \mathbb{R}$ satisfying $0 \leq r \leq s \leq k+1$, where the hidden constant depend only on k and the shape regularity constant ρ (cf. Assumption (**A1**)).*

We have the following trace estimate for curved domains, which is a particular case of [15, Theorem 3.4], with $\varepsilon = 0$.

Lemma 3.2 *Under the assumptions (**A0**) $-$ (**A2**), for all $E \in \Omega_h$ and $v \in H^1(E)$, it holds*

$$|v|_{1/2,\partial E} \lesssim |v|_{1,E}.$$

The hidden constant in the previous estimate depends only on the shape regularity constant ρ and $\|\gamma'\|_{L^\infty}$, in particular such constant does not depend on h_E.

The following result establishes the extension of the scaled trace theorem over straight to curved polygons.

Lemma 3.3 *For all $E \in \Omega_h$, the following scaled trace inequalities hold*

$$\|v\|_{0,\partial E}^2 \lesssim h_E^{-1} \|v\|_{0,E}^2 + h_E |v|_{1,E}^2 \qquad \forall v \in H^1(E),$$
$$|v|_{1,\partial E}^2 \lesssim h_E^{-1} |v|_{1,E}^2 + |v|_{3/2,E}^2 \qquad \forall v \in H^{3/2}(E),$$

where the hidden constants depend only on the shape regularity constant ρ and γ' (in particular it does not depend on h_E).

Proof. The proof follows from by combining the trace and Young inequalities, along with the arguments of [15, Lemma 3.4] (see also [20]).

$\square$

We finally state the following well-known Poincaré–Friedrichs inequalities on Lipschitz domains.

$$h_E^{-1} \|v\|_{0,E} \lesssim |v|_{1,E} + h_E^{-1} \left| \int_{\partial E} v \, ds \right| \qquad\qquad \forall v \in H^1(E), \tag{3.1}$$

$$h_E^{-2} \|v\|_{0,E} \lesssim |v|_{2,E} + h_E^{-2} \left| \int_{\partial E} v \, ds \right| + h_E^{-1} \left| \int_{\partial E} \nabla v \, ds \right| \quad \forall v \in H^2(E). \tag{3.2}$$

We close this section by recalling the properties of the Stein extension operator $\widetilde{\mathcal{E}}$ in [44, Chapter VI, Theorem 5'].

Lemma 3.4 *Given a Lipschitz domain $\Omega \subset \mathbb{R}^2$ and $t \in \mathbb{R}$ an non-negative real number, there exists an extension operator $\widetilde{\mathcal{E}} : H^t(\Omega) \to H^t(\mathbb{R}^2)$ and a positive constant C_t such that*

$$\widetilde{\mathcal{E}}(v)|_\Omega = v \qquad and \qquad \|\widetilde{\mathcal{E}}(v)\|_{t,\mathbb{R}^2} \lesssim \|v\|_{t,\Omega} \quad \forall v \in H^t(\Omega),$$

where hidden constant depends on t but not on the diameter of Ω.

3.2 Interpolation results

We start by presenting a preliminary lemma concerning only the approximation properties on the boundary of elements.

Lemma 3.5 *Let $e \subset \partial E$ be an (possibly curved) edge of an element $E \in \Omega_h$ and let $v \in H^1(E)$ with $v|_{\partial E} \in C^1(\partial E)$. Let moreover $v|_e \in H^t(e)$, for $2 < t \le k+1$. Let $\widetilde{v}_I \in V_k^h(E)$ be the interpolant of v with respect to the boundary DoFs $\boldsymbol{D}^\partial$ introduced in Section 2.1. Then, for all $0 \le m \le t$ it holds*

$$|v - \widetilde{v}_I|_{m,e} \lesssim h_E^{t-m} \|v\|_{t,e}. \tag{3.3}$$

Moreover, for all $0 \le m \le t - 1$ we have

$$|\partial_{\mathbf{n}_E} v - \partial_{\mathbf{n}_E} \widetilde{v}_I|_{m,e} \lesssim h_E^{t-1-m} \|\partial_{\mathbf{n}_E} v\|_{t-1,e}. \tag{3.4}$$

The hidden constants in the two above estimates are independent of h_E.

Proof. Note that the result involves only the edges of the element and the associated boundary degrees of freedom. Therefore it is actually a one-dimensional approximation result for interpolants in mapped polynomial spaces. As a consequence, the proof easily follows by combining the arguments of [15, Lemma 3.2] and the definition of degrees of freedom $\boldsymbol{D}^\partial$. $\square$

Next result provides the construction of an interpolant (for a smooth enough function) in the virtual element space V_k^h defined in (2.4). Moreover, this result establishes the corresponding error estimate.

Theorem 3.1 *Under Assumptions $(\mathbf{A0}) - (\mathbf{A2})$, for all $v \in H^s(\Omega) \cap V$, with $2 < s \le k+1$, there exists $v_I \in V_k^h$ such that*

$$|v - v_I|_{2,\Omega} \le C \, h^{s-2} \|v\|_{s,\Omega},$$

where C is a positive constant which depends on the degree k, the shape regularity constant ρ and the parametrization γ.

Proof. Let $v \in H^s(\Omega) \cap V$, then for all $E \in \Omega_h$, we can choose the polynomial function $v_\pi \in \mathbb{P}_k(E)$, such that Lemma 3.1 it holds, i.e.,

$$|v - v_\pi|_{2,E} \lesssim h_E^{s-2} |v|_{s,E}. \tag{3.5}$$

Let us consider the following biharmonic problem: find $v_I \in H^2(E)$ such that

$$\begin{cases} \Delta^2 v_I = \Delta^2 v_\pi & \text{in } E, \\ v_I = \widetilde{v}_I & \text{on } \partial E, \\ \partial_{\mathbf{n}_E} v_I = \partial_{\mathbf{n}_E} \widetilde{v}_I & \text{on } \partial E, \end{cases}$$

10

where $\widetilde{v}_{\mathrm{I}}$ is the interpolant in Lemma 3.5. From the above definition we deduce that $v_{\mathrm{I}} \in V_k^h$. Moreover, the difference $(v_{\mathrm{I}} - v_\pi)|_E$ satisfies the following local problem

$$\begin{cases} \Delta^2(v_{\mathrm{I}} - v_\pi) = 0 & \text{in } E, \\ (v_{\mathrm{I}} - v_\pi) = (\widetilde{v}_{\mathrm{I}} - v_\pi) & \text{on } \partial E, \\ \partial_{\mathbf{n}_E}(v_{\mathrm{I}} - v_\pi) = \partial_{\mathbf{n}_E}(\widetilde{v}_{\mathrm{I}} - v_\pi) & \text{on } \partial E. \end{cases} \tag{3.6}$$

Now, we will introduce the following notation: for $i \in \{1, 3\}$, we consider the scaled norm $||| \cdot |||_{i/2,e}$ on e, defined by

$$|||\varphi|||_{i/2,e} := \left(h_E^{-i} \|\varphi\|_{0,e}^2 + |\varphi|_{i/2,e}^2 \right)^{1/2} \qquad \forall \varphi \in H^{i/2}(e).$$

Since $(v_{\mathrm{I}} - v_\pi)$ is biharmonic, from [34, Page 17], we deduce the following (scaled) continuous dependence on the data for problem (3.6)

$$|v_{\mathrm{I}} - v_\pi|_{2,E}^2 \lesssim \sum_{e \in \partial E} (|||\partial_{\mathbf{n}_E}(v_{\mathrm{I}} - v_\pi)|||_{1/2,e}^2 + |||v_{\mathrm{I}} - v_\pi|||_{3/2,e}^2) =: \sum_{e \in \partial E} (T_{1,e} + T_{2,e}), \tag{3.7}$$

where the hidden constant is uniform respect to the element E.

First, we will estimate the term $T_{1,e}$ in (3.7). Adding and subtracting $\partial_{\mathbf{n}_E} v$, then by using triangular inequality, Lemmas 3.3, 3.2 and 3.1, we have

$$\begin{aligned} T_{1,e} = |||\partial_{\mathbf{n}_E}(v_{\mathrm{I}} - v_\pi)|||_{1/2,e}^2 &\lesssim |||\partial_{\mathbf{n}_E}(v_{\mathrm{I}} - v)|||_{1/2,e}^2 + |||\partial_{\mathbf{n}_E}(v - v_\pi)|||_{1/2,e}^2 \\ &= |||\partial_{\mathbf{n}_E}(v - v_{\mathrm{I}})|||_{1/2,e}^2 + h_E^{-1}\|\nabla(v - v_\pi)\|_{0,e}^2 + |\nabla(v - v_\pi)|_{1/2,e}^2 \\ &\lesssim |||\partial_{\mathbf{n}_E}(v - v_{\mathrm{I}})|||_{1/2,e}^2 + h_E^{-1}(h_E^{-1}\|\nabla(v - v_\pi)\|_{0,E}^2 + h_E|\nabla(v - v_\pi)|_{1,E}^2) + |\nabla(v - v_\pi)|_{1,E}^2 \\ &\lesssim |||\partial_{\mathbf{n}_E}(v - \widetilde{v}_{\mathrm{I}})|||_{1/2,e}^2 + h_E^{2(s-2)}\|v\|_{s,E}^2, \end{aligned} \tag{3.8}$$

where we also used that $\partial_{\mathbf{n}_E} v_I = \partial_{\mathbf{n}_E} \widetilde{v}_{\mathrm{I}}$ on ∂E.

Next, we will study the first term in (3.8). Let us denote $\chi_e := \partial_{\mathbf{n}_E}(v - \widetilde{v}_{\mathrm{I}})|_e$; by using the Poincaré inequality in one dimension (note that χ_e vanishes at both endpoints of e) we obtain $\|\chi_e\|_{0,e}^{1/2} \lesssim h_E^{1/2}|\chi_e|_{1,e}^{1/2}$. Thus, by combining such observation and estimates (3.4), we get

$$|||\chi_e|||_{1/2,e} \lesssim |\chi_e|_{1/2,e} \lesssim |\partial_{\mathbf{n}_E} v - \partial_{\mathbf{n}_E} \widetilde{v}_{\mathrm{I}}|_{1/2,e} \lesssim h_e^{s-2}|\partial_{\mathbf{n}_E} v|_{s-3/2,e} \lesssim h_E^{s-2}\|\nabla v\|_{s-3/2,e}. \tag{3.9}$$

Now, we will distinguish two cases. If the edge e is straight, then we can apply a standard trace inequality to obtain

$$|||\chi_e|||_{1/2,e} \lesssim h_E^{s-2}\|\nabla v\|_{s-3/2,e} \lesssim h_E^{s-2}\|\nabla v\|_{s-1,E} \lesssim h_E^{s-2}\|v\|_{s,E}.$$

If the edge e is curved, then we keep the estimate (3.9). Therefore, we can deduce that

$$|||\partial_{\mathbf{n}_E}(v - \widetilde{v}_{\mathrm{I}})|||_{1/2,e}^2 \lesssim \begin{cases} h_E^{2(s-2)}\|v\|_{s,E}^2 & \text{if } e \text{ is straight,} \\ h_E^{2(s-2)}\|\nabla v\|_{s-3/2,e}^2 & \text{if } e \text{ is curved.} \end{cases} \tag{3.10}$$

Thus, from estimates (3.8) and (3.10), and adding over all the edges, we can infer

$$\sum_{e \in \partial E} T_{1,e} = \sum_{e \in \partial E} |||\partial_{\mathbf{n}_E}(v_{\mathrm{I}} - v_\pi)|||_{1/2,e}^2 \lesssim h_E^{2(s-2)}(\|v\|_{s,E}^2 + \|\nabla v\|_{s-3/2,\partial E \cap \Gamma}^2). \tag{3.11}$$

In this part, we will analyze the term $T_{2,e}$. By employing similar arguments as in $T_{1,e}$, we arrive

$$\begin{aligned} T_{2,e} := |||v_{\mathrm{I}} - v_\pi|||_{3/2,e}^2 &\lesssim |||v - v_{\mathrm{I}}|||_{3/2,e}^2 + |||v - v_\pi|||_{3/2,e}^2 \\ &= |||v - v_{\mathrm{I}}|||_{3/2,e}^2 + h_E^{-3}\|v - v_\pi\|_{0,e}^2 + |v - v_\pi|_{3/2,e}^2 \\ &= |||v - v_{\mathrm{I}}|||_{3/2,e}^2 + h_E^{-3}(h_E^{-1}\|v - v_\pi\|_{0,E}^2 + h_E|v - v_\pi|_{1,E}^2) + |v - v_\pi|_{1,E}^2 \\ &\lesssim |||v - \widetilde{v}_{\mathrm{I}}|||_{3/2,e}^2 + h_E^{2(s-2)}\|v\|_{s,E}^2. \end{aligned}$$

We observe that $(v - \widetilde{v}_{\mathrm{I}})|_e \in H^{3/2}(e)$ and thus, by recalling bound (3.3), we obtain

$$|v - \widetilde{v}_{\mathrm{I}}|_{3/2,e}^2 \lesssim h_E^{2(s-2)}\|v\|_{s-1/2,e}^2.$$

11

Following the same arguments as those used to obtain (3.11), we can deduce

$$\sum_{e \in \partial E} T_{2,e} = \sum_{e \in \partial E} |||v_I - v_\pi|||_{3/2,e}^2 \lesssim h_E^{2(s-2)}(\|v\|_{s,E}^2 + \|v\|_{s-1/2,\partial E \cap \Gamma}^2). \tag{3.12}$$

Now, we combine (3.7), (3.11) and (3.12), then summing over all the elements $E \in \Omega_h$, yields

$$\sum_{E \in \Omega_h} |v - v_I|_{2,E}^2 \lesssim h_E^{2(s-2)} \Big(\|v\|_{s,\Omega}^2 + \sum_{i=1}^N (\|v\|_{s-1/2,\Gamma_i}^2 + \|\nabla v\|_{s-3/2,\Gamma_i}^2) \Big),$$

from where it follows

$$|v - v_I|_{2,\Omega} \lesssim h^{s-2} \Big(\|v\|_{s,\Omega} + \sum_{i=1}^N (\|v\|_{s-1/2,\Gamma_i} + \|\nabla v\|_{s-3/2,\Gamma_i}) \Big). \tag{3.13}$$

For any curve $\Gamma_i \subset \partial\Omega$, let $\mathcal{D}_i$ be a domain in $\mathbb{R}^2$, with boundary $\partial\mathcal{D}_i \in C^{s-2,1}$, such that $\Gamma_i \subset \partial\mathcal{D}_i$. Thus, we apply the trace theorem for smooth domains [40], and by Lemma 3.4, we get

$$\|v\|_{s-1/2,\Gamma_i} = \|\widetilde{\mathcal{E}}(v)\|_{s-1/2,\Gamma_i} \le \|\widetilde{\mathcal{E}}(v)\|_{s-1/2,\partial\mathcal{D}_i} \le \|\widetilde{\mathcal{E}}(v)\|_{s,\mathcal{D}_i} \le \|\widetilde{\mathcal{E}}(v)\|_{s,\mathbb{R}^2} \lesssim \|v\|_{s,\Omega}.$$

Analogously, applying a vector valued version of the Stein extension operator in Lemma 3.4, we have

$$\|\nabla v\|_{s-3/2,\Gamma_i} = \|\widetilde{\mathcal{E}}(\nabla v)\|_{s-3/2,\Gamma_i} \lesssim \|\nabla v\|_{s-1,\Omega} \lesssim \|v\|_{s,\Omega}.$$

We obtain the desired result by combining the above estimates, the triangular inequality together with the bounds (3.13) and (3.5). $\qquad\square$

3.3 Stability analysis

In the present section we prove stability bounds of the bilinear form $\mathcal{S}_E$ introduced in (2.10). We start with the following result, which provides, in some sense, the continuity of the stabilizing form. Note that the involved space is the enlarged one (2.8).

Proposition 3.1 *Let $E \in \Omega_h$ and $\mathcal{S}_E(\cdot,\cdot)$ be the bilinear form defined in (2.10). Then, under assumptions $(\mathbf{A0}) - (\mathbf{A2})$, for all $w_h \in \mathbb{V}_k^h(E)$ we have the following property*

$$\mathcal{S}_E(w_h, w_h) \lesssim h_E^{-4} \|w_h\|_{0,E}^2 + |w_h|_{2,E}^2 + h_E |w_h|_{5/2,E}^2. \tag{3.14}$$

Moreover, if w_h and ∇w_h have zero average on ∂E, we deduce

$$\mathcal{S}_E(w_h, w_h) \lesssim |w_h|_{2,E}^2 + h_E |w_h|_{5/2,E}^2, \tag{3.15}$$

where the hidden constants are independent of h_E.

Proof. From definition (2.10), we have

$$\mathcal{S}_E(w_h, w_h) = \mathcal{S}_E^\circ(w_h, w_h) + \mathcal{S}_E^{\partial,\mathbf{v}}(w_h, w_h) + \mathcal{S}_E^{\partial,e}(w_h, w_h)$$

$$\approx h_E^{-2} \sum_{j=1}^{(k-3)(k-2)/2} \boldsymbol{D}_j^\circ(w_h)^2 + \sum_{i=1}^{3N_E} h_{\mathbf{v}_i}^{-2} \boldsymbol{D}_i^{\partial,\mathbf{v}}(w_h)^2 + h_E \sum_{i=1}^{N_e} |\nabla w_h|_{1,e}^2. \tag{3.16}$$

First, we will analyze the term $\mathcal{S}_E^\circ(w_h, w_h)$. Indeed, by recalling that the polynomial basis $\{m_j\}_{j=1}^{(k-3)(k-2)/2}$ in $\boldsymbol{D}^\circ$ satisfies $\|m_j\|_{L^\infty(E)} \le 1$, and using the Cauchy-Schwarz inequality we obtain

$$\mathcal{S}_E^\circ(w_h, w_h) = \sum_{j=1}^{(k-3)(k-2)/2} h_E^{-2} \Big(h_E^{-2} \int_E w_h \, m_j \, \mathrm{d}E \Big)^2$$

$$\le h_E^{-2} h_E^{-4} \Big(\int_E w_h \, \mathrm{d}E \Big)^2 \sum_{j=1}^{(k-3)(k-2)/2} \|m_j\|_{L^\infty(E)}^2 \tag{3.17}$$

$$\lesssim h_E^{-2} h_E^{-4} |E| \|w_h\|_{0,E}^2 \lesssim h_E^{-4} \|w_h\|_{0,E}^2.$$

Now, we will relabel the index for the term $\mathcal{S}^{\partial,\mathbf{v}}(w_h, w_h)$ (see DoFs $\boldsymbol{D}_{\boldsymbol{I}}^{\partial}$ and $\boldsymbol{D}_{\boldsymbol{II}}^{\partial}$), as follows

$$\mathcal{S}_E^{\partial,\mathbf{v}}(w_h, w_h) = \sum_{i_1=1}^{N_E} h_{\mathbf{v}_i}^{-2} \boldsymbol{D}_{i_1}^{\partial,\boldsymbol{I}}(w_h)^2 + \sum_{i_2=1}^{2N_E} h_{\mathbf{v}_i}^{-2} \boldsymbol{D}_{i_2}^{\partial,\boldsymbol{II}}(w)^2 =: \mathcal{S}_E^{\partial,\boldsymbol{I}}(w_h, w_h) + \mathcal{S}_E^{\partial,\boldsymbol{II}}(w_h, w_h). \qquad (3.18)$$

By using the Sobolev inequality [20, Equation (2.4)] and $h_{\mathbf{v}_{i_1}} \approx h_E$, we have

$$\begin{aligned}
\mathcal{S}_E^{\partial,\boldsymbol{I}}(w_h, w_h) &\lesssim N_E \, h_{\mathbf{v}_{i_1}}^{-2} \|w_h\|_{L^\infty(\partial E)}^2 \lesssim h_E^{-2} \|w_h\|_{L^\infty(E)}^2 \\
&\lesssim h_E^{-2}(h_E^{-2}\|w_h\|_{0,E}^2 + |w_h|_{1,E}^2 + h_E^2 |w_h|_{2,E}^2) \\
&\lesssim h_E^{-4}\|w_h\|_{0,E}^2 + h_E^{-2}|w_h|_{1,E}^2 + |w_h|_{2,E}^2.
\end{aligned} \qquad (3.19)$$

For the term $\mathcal{S}^{\partial,\boldsymbol{II}}(w_h, w_h)$, since $h_{\mathbf{v}_i} \approx h_E$ and $L^\infty(E)$ is continuously embedded in $H^{5/2}(E)$, we obtain

$$\mathcal{S}_E^{\partial,\boldsymbol{II}}(w_h, w_h) \lesssim 2N_E h_{\mathbf{v}_{i_1}}^{-2} h_{\mathbf{v}_i}^2 \|\nabla w_h\|_{L^\infty(E)}^2 \lesssim h_E^{-2}|w_h|_{1,E}^2 + h_E|w_h|_{5/2,E}^2. \qquad (3.20)$$

The uniformity (with respect to the polygon E) of the last bound in (3.20) can be derived by the same arguments presented in [15, Lemma 3.4] (map to the ball, apply the result, map back) applied to ∇w_h.

Now, by using the second trace inequality of Lemma 3.3, for the remaining term we have

$$\mathcal{S}_E^{\partial,e}(w_h, w_h) \lesssim h_E \sum_{i=1}^{N_e} |\nabla w_h|_{1,e}^2 \lesssim |\nabla w_h|_{1,E}^2 + h_E|\nabla w_h|_{3/2,E}^2 \lesssim |w_h|_{2,E}^2 + h_E|w_h|_{5/2,E}^2. \qquad (3.21)$$

Thus, by combining (3.17)-(3.21) and (3.16), we get

$$\mathcal{S}_E(w_h, w_h) \lesssim h_E^{-4}\|w_h\|_{0,E}^2 + h_E^{-2}|w_h|_{1,E}^2 + |w_h|_{2,E}^2 + h_E|w_h|_{5/2,E}^2. \qquad (3.22)$$

Next, we observe that

$$h_E^{-2}|w_h|_{1,E}^2 \lesssim h_E^{-2}|w_h - \Pi_E^1 w_h|_{1,E}^2 + h_E^{-2}|\Pi_E^1 w_h|_{1,E}^2 \lesssim |w_h|_{2,E}^2 + h_E^{-4}\|w_h\|_{0,E}^2,$$

where we have used approximation and stability properties of projection Π_E^1 along with an inverse inequality for polynomials. From the above bound and (3.22), we conclude property (3.14).

The bound (3.15) follows from the Poincaré–Friedrichs inequality on Lipschitz domains (3.2). The proof is complete.

$\square$

Now, we recall the following result, which establishes a norm equivalence on polygons (see for instance [15]).

Lemma 3.6 *Let $E \in \Omega_h$. Under the assumptions $(\mathbf{A0}) - (\mathbf{A2})$, let $\mathbf{g} := (g_j)_{j=1}^{d_t}$ be a vector of real coefficients and let $g := \sum_j^{d_t} g_j \, m_j \in \mathbb{P}_t(E)$, where $d_t = \dim(\mathbb{P}_t(E))$. Then, the following norm equivalence holds*

$$h_E^2 \, \|\mathbf{g}\|_{\ell^2}^2 \lesssim \|g\|_{0,E}^2 \lesssim h_E^2 \, \|\mathbf{g}\|_{\ell^2}^2,$$

where the hidden constants are uniform and $\|\cdot\|_{\ell^2}$ is the classical ℓ^2-norm.

Additionally, we have the following H^2-orthogonality decomposition.

Lemma 3.7 *Any function $v_h \in H^2(E)$ admits the decomposition $v_h = v_1 + v_2$, where*

- $v_1 \in H^2(E)$, $v_1|_{\partial E} = v_h|_{\partial E}$, $\partial_{\mathbf{n}_E} v_1 = \partial_{\mathbf{n}_E} v_h$ and $\Delta^2 v_1 = 0 \quad in \quad E$;
- $v_2 \in H_0^2(E)$, $\Delta^2 v_2 = \Delta^2 v_h \quad in \quad E$.

Moreover, this decomposition is H^2-orthogonal in the sense that

$$|v_h|_{2,E}^2 = |v_1|_{2,E}^2 + |v_2|_{2,E}^2. \qquad (3.23)$$

13

Proof. Let $v_h \in H^2(E)$. We can choose v_2 as the H^2-projection of v_h in $H_0^2(E)$ and define $v_1 := v_h - v_2 \in H^2(E)$. We observe that by construction the functions v_1 and v_2 satisfy the properties of the lemma. $\qquad\square$

For any $e \in \partial E$ and $w_h \in H^{5/2}(E)$ the following Poincaré-type estimate in one-dimension is easy to check

$$\|w_h\|_{0,e}^2 \lesssim h_E^2 |w_h|_{1,e}^2 + h_E |w_h(\mathbf{v}_e^i)|^2 \qquad \text{and} \qquad |w_h|_{1,e}^2 \lesssim h_E^2 |w_h|_{2,e}^2 + h_E |\nabla w_h(\mathbf{v}_e^i)|^2,$$

where $\mathbf{v}_e^i$ is an extremal point of e. Thus, we can deduce that

$$h_E^{-3} \|w_h\|_{0,e}^2 \lesssim h_E^{-1} |w_h|_{1,e}^2 + h_E^{-2} |w_h(\mathbf{v}_e^i)|^2, \qquad \text{and} \qquad h_E^{-1} |w_h|_{1,e}^2 \lesssim h_E |w_h|_{2,e}^2 + |\nabla w_h(\mathbf{v}_e^i)|^2,$$

which implies

$$h_E^{-3} \|w_h\|_{0,e}^2 + h_E^{-1} |w_h|_{1,e}^2 \lesssim h_E |w_h|_{2,e}^2 + |\nabla w_h(\mathbf{v}_e^i)|^2 + h_E^{-2} |w_h(\mathbf{v}_e^i)|^2.$$

Moreover, by analogous arguments

$$h_E^{-1} \|\partial_{\mathbf{n}_E} w_h\|_{0,e}^2 \lesssim h_E |\partial_{\mathbf{n}_E} w_h|_{1,e}^2 + |\nabla w_h(\mathbf{v}_e^i)|^2.$$

From the above bound and the definition of $\mathcal{S}_E(\cdot,\cdot)$ we can conclude that for all $w_h \in H^{5/2}(E)$ it holds

$$\mathcal{S}_E(w_h, w_h) \gtrsim \sum_{e \in \partial E} \left(h_E^{-1} \|\partial_{\mathbf{n}_E} w_h\|_{0,e}^2 + h_E |\partial_{\mathbf{n}_E} w_h|_{1,e}^2 + h_E^{-3} \|w_h\|_{0,e}^2 + h_E^{-1} |w_h|_{1,e}^2 + h_E |w_h|_{2,e}^2 \right). \tag{3.24}$$

The above property will be fundamental to prove the coercivity of the stabilizing form $\mathcal{S}_E(\cdot,\cdot)$ in the space $V_k^h(E) + \mathbb{P}_1(E)$, which is established in the following result.

Lemma 3.8 *Under Assumptions* $(\mathbf{A0}) - (\mathbf{A2})$ *it holds*

$$\mathcal{S}_E(v_h, v_h) \gtrsim |v_h|_{2,E}^2 \qquad \forall v_h \in V_k^h(E) + \mathbb{P}_1(E), \quad \text{and} \quad \forall E \in \Omega_h,$$

where the hidden constant is independent of h_E.

Proof. Let $v_h \in V_k^h(E) + \mathbb{P}_1(E)$ and $v_1 \in H^2(E)$ and $v_2 \in H_0^2(E)$ such that Lemma 3.7 holds true. First, we will show that $|v_1|_{2,E}^2 \lesssim \mathcal{S}_E(v_h, v_h)$. Indeed, as in (3.7) we use the continuous dependence of the data and the construction of v_1, as follows

$$|v_1|_{2,E}^2 \lesssim \sum_{e \in \partial E} (|||\partial_{\mathbf{n}_E} v_h|||_{1/2,e}^2 + |||v_h|||_{3/2,e}^2) =: \sum_{e \in \partial E} (T_{1,e} + T_{2,e}). \tag{3.25}$$

Using property (3.24), we immediately obtain

$$h_E^{-1} \|\partial_{\mathbf{n}_E} v_h\|_{0,e}^2 \lesssim \mathcal{S}_E(v_h, v_h).$$

Now, by employing the real interpolation method, the Young inequality, and again property (3.24), we get

$$|\partial_{\mathbf{n}_E} v_h|_{1/2,e}^2 \lesssim \|\partial_{\mathbf{n}_E} v_h\|_{0,e} |\partial_{\mathbf{n}_E} v_h|_{1,e} \lesssim h_E^{-1} \|\partial_{\mathbf{n}_E} v_h\|_{0,e}^2 + h_E |\partial_{\mathbf{n}_E} v_h|_{1,e}^2 \lesssim \mathcal{S}_E(v_h, v_h).$$

Therefore, for the term $T_{1,e}$, we have the following bound

$$T_{1,e} = |||\partial_{\mathbf{n}_E} v_h|||_{1/2,e}^2 = h_E^{-1} \|\partial_{\mathbf{n}_E} v_h\|_{0,e}^2 + |\partial_{\mathbf{n}_E} v_h|_{1/2,e}^2 \lesssim \mathcal{S}_E(v_h, v_h). \tag{3.26}$$

Analogously, we can derive

$$h_E^{-3} \|v_h\|_{0,e}^2 \lesssim \mathcal{S}_E(v_h, v_h) \qquad \text{and} \quad |v_h|_{3/2,e}^2 \lesssim |v_h|_{1,e} |v_h|_{2,e} \lesssim \mathcal{S}_E(v_h, v_h).$$

Thus, by combining the above estimates we have

$$T_{2,e} = |||v_h|||_{3/2,e}^2 = h_E^{-3} \|v_h\|_{0,e}^2 + |v_h|_{3/2,e}^2 \lesssim \mathcal{S}_E(v_h, v_h). \tag{3.27}$$

Inserting (3.26) and (3.27) in (3.25), we conclude

$$|v_1|_{2,E}^2 \lesssim \mathcal{S}_E(v_h, v_h). \tag{3.28}$$

14

Now, we will analyze the second part of the decomposition. Indeed, let $g := \Delta^2 v_h = \Delta^2 v_2 \in \mathbb{P}_{k-4}(E)$, then using the fact that $v_h = v_1 + v_2$ and an integration by parts, it follows that

$$|v_2|^2_{2,E} = \int_E v_2 \Delta^2 v_2 = \int_E g v_2 = \int_E g v_h - \int_E g v_1 =: T_{1,E} + T_{2,E}. \tag{3.29}$$

Since $g \in \mathbb{P}_{k-4}(E)$, then we can write

$$g = \sum_{j=1}^{(k-3)(k-2)/2} g_j m_j.$$

Then, from the definition of $\boldsymbol{D}^\circ$, the Cauchy-Schwarz inequality for sequences, Lemma 3.6, and the first term can be bounded as follows

$$T_{1,E} = \int_E g v_h = \sum_{j=1}^{(k-3)(k-2)/2} g_j \int_E m_j v_h \mathrm{d}E = \sum_{j=1}^{(k-3)(k-2)/2} h_E^2 g_j \, \boldsymbol{D}^\circ_j(v_h)$$

$$\lesssim h_E^3 \left(\sum_{j=1}^{(k-3)(k-2)/2} g_j^2 \right)^{1/2} \left(\sum_{j=1}^{(k-3)(k-2)/2} h_E^{-2} \boldsymbol{D}^\circ_j(v_h)^2 \right)^{1/2}$$

$$\lesssim h_E^3 \|\mathbf{g}\|_{\ell^2} \, \mathcal{S}^\circ_E(v_h, v_h)^{1/2}$$

$$\lesssim h_E^2 \|\Delta^2 v_2\|_{0,E} \, \mathcal{S}_E(v_h, v_h)^{1/2}.$$

We now observe that, exploiting that $\Delta^2 v_2$ is a polynomial function in E, we can apply similar arguments of Lemma 6.3 in [14] leading to

$$\|\Delta^2 v_2\|_{0,E} \lesssim h_E^{-2} |v_2|_{2,E}. \tag{3.30}$$

Thus,

$$T_{1,E} \lesssim |v_2|_{2,E} \, \mathcal{S}_E(v_h, v_h)^{1/2}. \tag{3.31}$$

On the other hand, by applying again the Cauchy-Schwarz and (3.30) we have

$$T_{2,E} = \int_E g v_1 \le \|\Delta^2 v_2\|_{0,E} \|v_1\|_{0,E} \lesssim h_E^{-2} |v_2|_{2,E} \|v_1\|_{0,E}. \tag{3.32}$$

The goal now is to show that $h_E^{-2} \|v_1\|_{0,E} \lesssim \mathcal{S}_E(v_h, v_h)^{1/2}$. In order to achieve that, recalling that on ∂E it holds $v_h = v_1$, $\partial_{\mathbf{n}_E} v_h = \partial_{\mathbf{n}_E} v_1$, we first start applying the Poincaré–Friedrichs inequality (3.2) and Hölder inequality, then continue using (3.24), and (3.28). We obtain

$$\|v_1\|_{0,E} \lesssim h_E^2 |v_1|_{2,E} + \left| \int_{\partial E} v_1 \, \mathrm{d}s \right| + h_E \left| \int_{\partial E} \nabla v_1 \, \mathrm{d}s \right|$$

$$\lesssim h_E^2 |v_1|_{2,E} + h_E^{1/2} \|v_h\|_{0,\partial E} + h_E^{3/2} |v_h|_{1,\partial E}$$

$$\lesssim h_E^2 |v_1|_{2,E} + h_E^2 \, \mathcal{S}_E(v_h, v_h)^{1/2}$$

$$\lesssim h_E^2 \, \mathcal{S}_E(v_h, v_h)^{1/2}.$$

Then, from the above bound and (3.32), we conclude

$$T_{2,E} \lesssim |v_2|_{2,E} \, \mathcal{S}_E(v_h, v_h)^{1/2}.$$

Therefore, by combining (3.31), the above estimate, and (3.29), it follows that

$$|v_2|^2_{2,E} \lesssim \mathcal{S}_E(v_h, v_h). \tag{3.33}$$

Finally, the desired result follows inserting (3.28) and (3.33) in (3.23).

$$\square$$

We have the following stability result.

Proposition 3.2 *There exists a positive uniform constant α_* such that for any element $E \in \Omega_h$ it holds*

$$a_E^h(v_h, \, v_h) \ge \alpha_* \, a_E(v_h, \, v_h) \quad \forall v_h \in V_k^h(E).$$

As a consequence the global bilinear form $a^h(\cdot, \cdot)$ is coercive.

Proof. In order to simplify the notation, we temporarily denote by $\overline{\Pi}_E := \Pi_E^{\mathbf{D},1}$, which is the operator defined in (2.5) for the particular case $k = 1$. Such operator, acting from $V_k^h(E)$ onto $\mathbb{P}_1(E)$, preserves by construction the boundary integral of the function and its gradient.

Let $v_h \in V_k^h(E)$, then we set $\widetilde{v} := (v_h - \overline{\Pi}_E v_h) \in V_k^h(E) + \mathbb{P}_1(E)$. First, we note that from definitions (2.5) and (2.6) we deduce $(I - \Pi_E^{\mathbf{D},k})\widetilde{v} = (I - \Pi_E^{\mathbf{D},k})v_h$. Now, by employing Lemma 3.8, some algebraic manipulations and the above observation, we obtain

$$
\begin{aligned}
a_E(v_h, v_h) = a_E(\widetilde{v}, \widetilde{v}) &\lesssim \mathcal{S}_E(\widetilde{v}, \widetilde{v}) \lesssim \mathcal{S}_E(\Pi_E^{\mathbf{D},k}\widetilde{v}, \Pi_E^{\mathbf{D},k}\widetilde{v}) + \mathcal{S}_E((I - \Pi_E^{\mathbf{D},k})\widetilde{v}, (I - \Pi_E^{\mathbf{D},k})\widetilde{v}) \\
&= \mathcal{S}_E(\Pi_E^{\mathbf{D},k}\widetilde{v}, \Pi_E^{\mathbf{D},k}\widetilde{v}) + \mathcal{S}_E((I - \Pi_E^{\mathbf{D},k})v_h, (I - \Pi_E^{\mathbf{D},k})v_h).
\end{aligned}
\tag{3.34}
$$

By construction we have $(\widetilde{v}, 1)_{0,\partial E} = (\nabla \widetilde{v}, 1)_{0,\partial E} = 0$, thus we conclude $(\Pi_E^{\mathbf{D},k}\widetilde{v}, 1)_{0,\partial E} = (\nabla \Pi_E^{\mathbf{D},k}\widetilde{v}, 1)_{0,\partial E} = 0$. Then, by using property (3.15) of Proposition 3.1, we get

$$
\mathcal{S}_E(\Pi_E^{\mathbf{D},k}\widetilde{v}, \Pi_E^{\mathbf{D},k}\widetilde{v}) \lesssim |\Pi_E^{\mathbf{D},k}\widetilde{v}|_{2,E}^2 + h_E |\Pi_E^{\mathbf{D},k}\widetilde{v}|_{5/2,E}^2.
$$

Now, we observe that inserting the above bound in (3.34) we can infer

$$
a_E(v_h, v_h) \lesssim |\Pi_E^{\mathbf{D},k}\widetilde{v}|_{2,E}^2 + h_E |\Pi_E^{\mathbf{D},k}\widetilde{v}|_{5/2,E}^2 + \mathcal{S}_E((I - \Pi_E^{\mathbf{D},k})v_h, (I - \Pi_E^{\mathbf{D},k})v_h).
\tag{3.35}
$$

By using standard polynomial inverse inequality on star-shaped polygons we have

$$
h_E |\Pi_E^{\mathbf{D},k}\widetilde{v}|_{5/2,E}^2 \lesssim |\Pi_E^{\mathbf{D},k}\widetilde{v}|_{2,E}^2.
$$

Moreover, from definition of operator $\Pi_E^{\mathbf{D},k}$ in (2.5), we easily observe that $|\Pi_E^{\mathbf{D},k}\widetilde{v}|_{2,E}^2 = |\Pi_E^{\mathbf{D},k}v_h|_{2,E}^2$. Therefore, by combining the above facts and (3.35), we obtain the desired result. $\qquad\square$

Remark 3.1 *We recall that the space $V_k^h(E)$ does not contain the kernel of $a_E(\cdot, \cdot)$, i.e., $\mathbb{P}_1(E) \not\subset V_k^h(E)$ (see Remark 2.2 and (2.5)). However, due to Lemma 3.8 it is still possible to obtain the first inequality in estimate (3.34), hence the coercivity of the discrete bilinear form $a_E^h(\cdot, \cdot)$. The aforementioned fact together with Remark 2.3 are our main motivations for introducing the new stabilization term $\mathcal{S}_E(\cdot, \cdot)$ (cf. (2.9)).*

3.4 A priori error estimates

In this section we will provide an a priori error analysis for our conforming virtual element scheme. We start recalling a bound for the load approximation error. We omit the simple proof since it follows from standard VEM arguments, see for instance [21].

Proposition 3.3 *Let $2 < s \le k + 1$ and*

$$
\alpha = \begin{cases} 0 & \text{if } k = 2, 3, \\ 1 & \text{if } k = 4, \\ k - 3 & \text{if } k > 4 \text{ and } s > 3. \end{cases}
\tag{3.36}
$$

*Then, under assumptions (**A1**)-(**A2**) and $f \in H^\alpha(\Omega)$, we have the following estimate*

$$
\|f - f_h\| := \sup_{v_h \in V_k^h} \frac{|(f, v_h)_{0,\Omega} - \langle f_h, v_h \rangle|}{|v_h|_{2,\Omega}} \lesssim h^{s-2} |f|_{\alpha,\Omega}.
$$

Next, for all $v \in H^s(\Omega)$ with $s > 2$, we introduce the following quantity:

$$
T^h(v) := \left(\sum_{E \in \Omega_h} a_E^h(v_\pi - v_\mathrm{I}, v_\pi - v_\mathrm{I}) \right)^{1/2},
\tag{3.37}
$$

where $v_\mathrm{I} \in V_k^h$ and $v_\pi \in \mathbb{P}_k(\Omega_h)$ are the VEM interpolant and polynomial projection of v in the sense of Theorem 3.1 and Lemma 3.1, respectively.

Remark 3.2 *The term $T^h(\cdot)$ defined in (3.37) will appear in the abstract error estimate below and is related to the VEM approximation of the bilinear form of the problem. A difficulty in bounding this term lies in the fact that we cannot directly use standard arguments since the norm appearing on the right-hand side of the continuity bound (3.15) is stronger than the norm in which we derived approximation estimates; compare Theorem 3.1 and Proposition 3.1. We provide an error bound for $T^h(u)$ in Lemma 3.9.*

The following result establishes an error estimate for the consistency term defined in (3.37).

Lemma 3.9 *Let $u \in V$ be the solution of problem (1.2) and assume that $u \in H^s(\Omega)$, with $5/2 \le s \le k+1$. Then, the following estimate holds*

$$T^h(u) \lesssim h^{s-2}\|u\|_{s,\Omega}.$$

Proof. By using the definition of $a_E^h(\cdot,\cdot)$ and $\mathcal{S}_E(\cdot,\cdot)$ we obtain

$$a_E^h(u_\pi - u_{\mathrm{I}},\, u_\pi - u_{\mathrm{I}}) \lesssim |u_\pi - u_{\mathrm{I}}|_{2,E}^2 + \mathcal{S}_E((I - \Pi_E^{\mathbf{D},k})(u_\pi - u_{\mathrm{I}}), (I - \Pi_E^{\mathbf{D},k})(u_\pi - u_{\mathrm{I}}))$$
$$= |u_\pi - u_{\mathrm{I}}|_{2,E}^2 + \mathcal{S}_E^\circ((I - \Pi_E^{\mathbf{D},k})u_{\mathrm{I}}, (I - \Pi_E^{\mathbf{D},k})u_{\mathrm{I}}) + \mathcal{S}_E^\partial((I - \Pi_E^{\mathbf{D},k})u_{\mathrm{I}}, (I - \Pi_E^{\mathbf{D},k})u_{\mathrm{I}}).$$

For simplicity, we denote $\overline{u}_{\mathrm{I}} := (I - \Pi_E^{\mathbf{D},k})u_{\mathrm{I}}$, then from (3.17), (3.18) and (3.19), we have

$$\mathcal{S}_E^\circ((I - \Pi_E^{\mathbf{D},k})u_{\mathrm{I}}, (I - \Pi_E^{\mathbf{D},k})u_{\mathrm{I}}) + \mathcal{S}_E^\partial((I - \Pi_E^{\mathbf{D},k})u_{\mathrm{I}}, (I - \Pi_E^{\mathbf{D},k})u_{\mathrm{I}})$$
$$\le h_E^{-4}\|\overline{u}_{\mathrm{I}}\|_{0,E}^2 + h_E^{-2}|\overline{u}_{\mathrm{I}}|_{1,E}^2 + |\overline{u}_{\mathrm{I}}|_{2,E}^2 + \mathcal{S}_E^{\partial,\mathit{\Pi}}(\overline{u}_{\mathrm{I}}, \overline{u}_{\mathrm{I}}) + \mathcal{S}_E^{\partial,e}(\overline{u}_{\mathrm{I}}, \overline{u}_{\mathrm{I}}).$$

By definition $\Pi_{\partial E}^0 \overline{u}_{\mathrm{I}} = \Pi_{\partial E}^0(\nabla \overline{u}_{\mathrm{I}}) = 0$, thus by combining the two above estimates and the Poincaré–Friedrichs inequality (cf. (3.2)), it follows that

$$a_E^h(u_\pi - u_{\mathrm{I}},\, u_\pi - u_{\mathrm{I}}) \lesssim |u_\pi - u_{\mathrm{I}}|_{2,E}^2 + |\overline{u}_{\mathrm{I}}|_{2,E}^2 + \mathcal{S}_E^{\partial,\mathit{\Pi}}(\overline{u}_{\mathrm{I}}, \overline{u}_{\mathrm{I}}) + \mathcal{S}_E^{\partial,e}(\overline{u}_{\mathrm{I}}, \overline{u}_{\mathrm{I}})$$
$$=: T_1^E + T_2^E + T_3^E + T_4^E. \tag{3.38}$$

By using the triangle inequality, for the first term, we get

$$T_1^E \lesssim |u_\pi - u|_{2,E}^2 + |u - u_{\mathrm{I}}|_{2,E}^2. \tag{3.39}$$

Concerning the term T_2^E, by the continuity of the operator $\Pi_E^{\mathbf{D},k}$ we obtain

$$T_2^E = |(I - \Pi_E^{\mathbf{D},k})u_{\mathrm{I}}|_{2,E}^2 \lesssim |(I - \Pi_E^{\mathbf{D},k})(u - u_{\mathrm{I}})|_{2,E}^2 + |(I - \Pi_E^{\mathbf{D},k})u|_{2,E}^2 \lesssim |u - u_{\mathrm{I}}|_{2,E}^2 + |u - u_\pi|_{2,E}^2. \tag{3.40}$$

Now, we will analyze the term T_3^E. By definition we have

$$T_3^E = \sum_{i_2=1}^{2N_E} h_{i_2}^{-2} \mathbf{D}_{i_2}^{\partial,\mathit{\Pi}}(\overline{u}_{\mathrm{I}})^2 = \sum_{i_2=1}^{2N_E} h_{i_2}^{-2} \mathbf{D}_{i_2}^{\partial,\mathit{\Pi}}(u - \Pi_E^{\mathbf{D},k}u_{\mathrm{I}})^2$$
$$\lesssim \|\nabla(u - \Pi_E^{\mathbf{D},k}u_{\mathrm{I}})\|_{L^\infty(E)}^2 \lesssim \|\nabla(u - \Pi_E^{\mathbf{D},k}u)\|_{L^\infty(E)}^2 + \|\nabla\Pi_E^{\mathbf{D},k}(u - u_{\mathrm{I}})\|_{L^\infty(E)} =: T_{3,1}^E + T_{3,2}^E.$$

By adding and subtracting u_π, then using the continuous embedding of $L^\infty(E)$ in $H^{1+\epsilon}(E)$, along with standard inverse inequality for polynomials on star-shaped polygons we deduce

$$T_{3,1}^E \le \|\nabla(u - u_\pi)\|_{L^\infty(E)}^2 + \|\nabla\Pi_E^{\mathbf{D},k}(u_\pi - u)\|_{L^\infty(E)}^2$$
$$\lesssim h_E^{-2}|u - u_\pi|_{1,E}^2 + h^{2(s-2)}|u - u_\pi|_{s,E}^2 + h_E^{-2}\|\nabla\Pi_E^{\mathbf{D},k}(u_\pi - u)\|_{0,E}^2$$
$$\lesssim |u - u_\pi|_{2,E}^2 + h^{2(s-2)}|u - u_\pi|_{s,E}^2 + |\Pi_E^{\mathbf{D},k}(u_\pi - u)|_{2,E}^2$$
$$\lesssim |u - u_\pi|_{2,E}^2 + h^{2(s-2)}|u - u_\pi|_{s,E}^2,$$

where we also used Lemma 3.1, and the continuity of projection $\Pi_E^{\mathbf{D},k}$ respect to the seminorm $|\cdot|_{2,E}$ in the second and last step, respectively.

Next, we will bound term $T_{3,2}^E$. By using the inverse and Poincaré–Friedrichs inequality (3.1), we obtain

$$T_{3,2}^E = \|\nabla\Pi_E^{\mathbf{D},k}(u - u_{\mathrm{I}})\|_{L^\infty(E)}^2 \lesssim h_E^{-2}\|\nabla\Pi_E^{\mathbf{D},k}(u - u_{\mathrm{I}})\|_{0,E}^2$$
$$\lesssim h_E^{-2}\|\nabla\Pi_E^{\mathbf{D},k}(u - u_{\mathrm{I}}) - \nabla(u - u_{\mathrm{I}})\|_{0,E}^2 + h_E^{-2}\|\nabla(u - u_{\mathrm{I}})\|_{0,E}^2$$
$$\lesssim |\nabla\Pi_E^{\mathbf{D},k}(u - u_{\mathrm{I}}) - \nabla(u - u_{\mathrm{I}})|_{1,E}^2 + h_E^{-2}\|\nabla(u - u_{\mathrm{I}})\|_{0,E}^2$$
$$\lesssim |u - u_{\mathrm{I}}|_{2,E}^2 + h_E^{-2}\|\nabla(u - u_{\mathrm{I}})\|_{0,E}^2,$$

17

where we have used also the continuity of projection $\Pi_E^{\mathbf{D},k}$ respect to the seminorm $|\cdot|_{2,E}$.

Now, by using again the Poincaré–Friedrichs inequality (3.1), splitting the gradient in tangent and normal components (and recalling that the integral on each edge of the tangent derivative of $u - u_I$ vanishes since such function is zero at all vertexes) we have

$$
\begin{aligned}
h_E^{-1}\|\nabla(u - u_I)\|_{0,E} &\lesssim |\nabla(u - u_I)|_{1,E} + h_E^{-1}\left|\int_{\partial E} \nabla(u - u_I)\,\mathrm{d}s\right| \\
&\lesssim |\nabla(u - u_I)|_{1,E} + h_E^{-1}\left|\int_{\partial E} \partial_{\mathbf{n}_E}(u - u_I)\,\mathrm{d}s\right| \\
&\lesssim |u - u_I|_{2,E} + h_E^{-1/2}\|\partial_{\mathbf{n}_E}(u - u_I)\|_{0,\partial E}.
\end{aligned}
$$

By employing Lemma 3.5, we have that

$$
h_E^{-1/2}\|\partial_{\mathbf{n}_E}(u - u_I)\|_{0,e} \lesssim h_E^{s-2}\|\partial_{\mathbf{n}_E}u\|_{s-3/2,e},
$$

and thus we easily derive, by the same argument used in Theorem 3.1,

$$
T_{3,2}^E \lesssim |u - u_I|_{2,E}^2 + h_E^{2(s-2)}\|\nabla u\|_{s-3/2,\partial E \cap \Gamma}^2.
$$

By collecting the bounds involving $T_{3,1}^E$ and $T_{3,2}^E$ we conclude

$$
T_3^E \lesssim h^{2(s-2)}|u - u_\pi|_{s,E}^2 + |u - u_\pi|_{2,E}^2 + |u - u_I|_{2,E}^2 + h_E^{2(s-2)}\|\nabla u\|_{s-3/2,\partial E \cap \Gamma}^2. \tag{3.41}
$$

By adding and subtracting suitable terms, we have that

$$
\begin{aligned}
T_4^E &\lesssim \sum_{e \in \partial E} h_E|\nabla \overline{u}_I|_{1,e}^2 \lesssim h_E \sum_{e \in \partial E}\left(|\nabla(u_I - u_\pi)|_{1,e}^2 + |\nabla(u_\pi - \Pi_E^{\mathbf{D},k}u)|_{1,e}^2 + |\nabla \Pi_E^{\mathbf{D},k}(u - u_I)|_{1,e}^2\right) \\
&=: h_E \sum_{e \in \partial E}(T_{4,1}^e + T_{4,2}^e + T_{4,3}^e).
\end{aligned} \tag{3.42}
$$

For the term $T_{4,1}^e$, we proceed applying the second trace inequality in Lemma 3.3, as follow

$$
\begin{aligned}
T_{4,1}^e &\lesssim |\nabla(u_I - u)|_{1,e}^2 + |\nabla(u - u_\pi)|_{1,e}^2 \\
&\lesssim |u_I - u|_{2,e}^2 + h_E^{-1}|\nabla(u - u_\pi)|_{1,E}^2 + |\nabla(u - u_\pi)|_{3/2,E}^2 \\
&\lesssim h^{2(s-5/2)}\|u\|_{s-1/2,e}^2 + h_E^{-1}|u - u_\pi|_{2,E}^2 + |u - u_\pi|_{5/2,E}^2,
\end{aligned} \tag{3.43}
$$

where we have applied Lemmas 3.5 in the first term.

Next, for the term $T_{4,2}^e$, we apply again the scaled trace bound in Lemma 3.3, to obtain

$$
\begin{aligned}
T_{4,2}^e = |\nabla(u_\pi - \Pi_E^{\mathbf{D},k}u)|_{1,e}^2 &\lesssim h_E^{-1}|\nabla(u_\pi - \Pi_E^{\mathbf{D},k}u)|_{1,E}^2 + |\nabla(u_\pi - \Pi_E^{\mathbf{D},k}u)|_{3/2,E}^2 \\
&\lesssim h_E^{-1}|\Pi_E^{\mathbf{D},k}(u_\pi - u)|_{2,E}^2 + |\Pi_E^{\mathbf{D},k}(u_\pi - u)|_{5/2,E}^2.
\end{aligned}
$$

From the above estimate, we observe that if $k = 2$, then $|\Pi_E^{\mathbf{D},k}(u_\pi - u)|_{5/2,E}^2 = 0$. However, if $k \geq 3$, then we can apply a classical inverse inequality for polynomials on star-shaped polygons, to obtain $|\Pi_E^{\mathbf{D},k}(u_\pi - u)|_{5/2,E}^2 \lesssim h_E^{-1}|\Pi_E^{\mathbf{D},k}(u_\pi - u)|_{2,E}^2$. Therefore, by using the continuity of the projection $\Pi_E^{\mathbf{D},k}$ respect with $|\cdot|_{2,E}$ for both cases, we get

$$
T_{4,2}^e \lesssim h_E^{-1}|u_\pi - u|_{2,E}^2. \tag{3.44}
$$

Following similar arguments we can derive

$$
T_{4,3}^e \lesssim h_E^{-1}|u - u_I|_{2,E}^2. \tag{3.45}
$$

By inserting (3.43)-(3.45) in (3.42), we obtain

$$
T_4^E \lesssim |u - u_\pi|_{2,E}^2 + |u - u_I|_{2,E}^2 + h_E|u - u_\pi|_{5/2,E}^2 + h_E^{2(s-2)}\|u\|_{s-1/2,\partial E \cap \Gamma}^2. \tag{3.46}
$$

By combining (3.39), (3.40), (3.41), (3.46), and (3.38), it follows that

$$a_E^h(u_\pi - u_I, u_\pi - u_I) \lesssim h^{2(s-2)}|u - u_\pi|_{s,E}^2 + h_E|u - u_\pi|_{5/2,E}^2 + |u - u_\pi|_{2,E}^2 + |u - u_I|_{2,E}^2 + h_E^{2(s-2)}\|u\|_{s-1/2,\partial E \cap \Gamma}^2.$$

Finally, the desired result follows easily from definition (3.37) and the above estimate, by applying similar arguments to those used in the proof of Theorem 3.1, the Stein extension operator and the approximation properties in Lemma 3.1, and Theorem 3.1. $\qquad\square$

In the following result we state an abstract error analysis in the energy norm for scheme (2.13), which can be seen as a Strang-type lemma and allow us to obtain optimal error estimates.

Theorem 3.2 *Under assumptions* (**A0**)-(**A2**), *let* $u \in V$ *and* $u_h \in V_k^h$ *be the solutions of problems* (1.2) *and* (2.13), *respectively. Then, for all* $u_I \in V_k^h$ *and each* $u_\pi \in \mathbb{P}_k(\Omega_h)$, *we have*

$$|u - u_h|_{2,\Omega} \lesssim |u - u_I|_{2,\Omega} + |u - u_\pi|_{2,h} + \|f - f_h\| + T^h(u). \tag{3.47}$$

Furthermore, if $u \in H^s(\Omega)$ *and* $f \in H^\alpha(\Omega)$, *with* $5/2 \leq s \leq k+1$ *and* α *as in* (3.36). *Then, we have the following error estimate*

$$|u - u_h|_{2,\Omega} \lesssim h^{s-2}(\|u\|_{s,\Omega} + |f|_{\alpha,\Omega}),$$

where the hidden constants depend on the degree k, *the parametrization* γ *and the shape regularity constant* ρ, *but is independent of* h.

Proof. Let $u_I \in V_k^h$ and $u_\pi \in \mathbb{P}_k(\Omega_h)$, then we set $\delta_h := (u_h - u_I) \in V_k^h$. By following standard steps in VEM analysis [10], we have

$$a^h(\delta_h, \delta_h) = a^h(u_h - u_I, \delta_h) = (f_h - f, \delta_h) + \sum_{E \in \Omega_h} \left(a_E^h(u_\pi - u_I, \delta_h) + a_E(u - u_\pi, \delta_h)\right)$$

$$\lesssim \|f - f_h\| |\delta_h|_{2,\Omega} + \sum_{E \in \Omega_h} a_E^h(u_\pi - u_I, \delta_h) + |u - u_\pi|_{2,h} |\delta_h|_{2,\Omega}.$$

Now, since $a_E^h(\cdot, \cdot)$ is symmetric and applying the Cauchy-Schwarz and Young inequalities we get

$$\sum_{E \in \Omega_h} a_E^h(u_\pi - u_I, \delta_h) \leq \sum_{E \in \Omega_h} a_E^h(u_\pi - u_I, u_\pi - u_I)^{1/2} a_E^h(\delta_h, \delta_h)^{1/2}$$

$$\leq \sum_{E \in \Omega_h} \frac{1}{2} a_E^h(u_\pi - u_I, u_\pi - u_I) + \frac{1}{2} a^h(\delta_h, \delta_h).$$

Thus, from the above bounds, the Young inequality and Proposition 3.2 we easily obtain

$$\frac{\alpha_*}{4} |\delta_h|_{2,\Omega}^2 \lesssim \|f - f_h\|^2 + \sum_{E \in \Omega_h} a_E^h(u_\pi - u_I, u_\pi - u_I) + |u - u_\pi|_{2,h}^2.$$

Therefore the desired result follows from the above bound and the triangular inequality.

The proof of the second part follows by bounding the the terms on the right-hand side of (3.47), by means of Theorem 3.1, Lemma 3.1, Proposition 3.3 and Lemma 3.9. $\qquad\square$

4 Numerical experiments

In this section we report numerical examples to test the performance of the new C^1-VE scheme with curved edges. In particular, we study the convergence of the proposed method from the practical perspective, comparing with Theorem 3.2. Moreover, we check numerically that an approximation of the domain by using "straight VE" polygons, leads to a sub-optimal rate of convergence for $k \geq 3$, as is expected.

In order to compute the experimental errors between the exact solution u and the VEM solution u_h, we consider the following computable error quantities:

$$\text{Err}_i(u) := \frac{\left(\sum_{E \in \Omega_h} |u - \Pi_E^{\mathbf{D},k} u_h|_{i,E}^2\right)^{1/2}}{|u|_{i,\Omega}}, \quad \text{for} \quad i = 1, 2,$$

$$\text{Err}_0(u) := \frac{\left(\sum_{E \in \Omega_h} \|u - \Pi_E^{\mathbf{D},k} u_h\|_{0,E}^2\right)^{1/2}}{\|u\|_{0,\Omega}},$$

(4.1)

which converge with the same rate as the exact errors $|u - u_h|_{i,\Omega}$ (with $i = 1, 2$) and $\|u - u_h\|_{0,\Omega}$, respectively.

We consider the curved domain Ω described by

$$\Omega := \{(x, y) \in \mathbb{R}^2 : \quad 0 < x < 1, \quad \text{and} \quad g_{bt}(x) < y < g_{tp}(x)\}, \tag{4.2}$$

where g_{bt} and g_{tp} are given by

$$g_{bt}(x) := \frac{1}{20} \sin(\pi x) \qquad \text{and} \qquad g_{tp}(x) := 1 + \frac{1}{20} \sin(3\pi x),$$

see Figure 2. We assume that the curved boundaries Γ_{bt} and Γ_{tp} are given with the standard graph parametrization, which are given by (see [15]),

$$\gamma_{bt} : [0, 1] \rightarrow \Gamma_{bt} \qquad \gamma_{bt}(t) = \left(t, \frac{1}{20} \sin(\pi t) \right),$$

$$\gamma_{tp} : [0, 1] \rightarrow \Gamma_{tp} \qquad \gamma_{tp}(t) = \left(t, 1 + \frac{1}{20} \sin(3\pi t) \right).$$
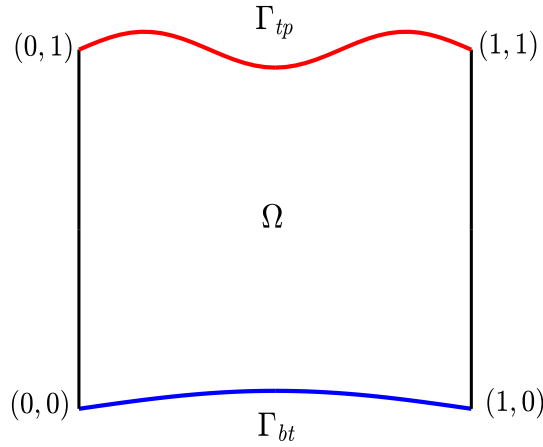
Figure 2: The domain Ω described in (4.2).
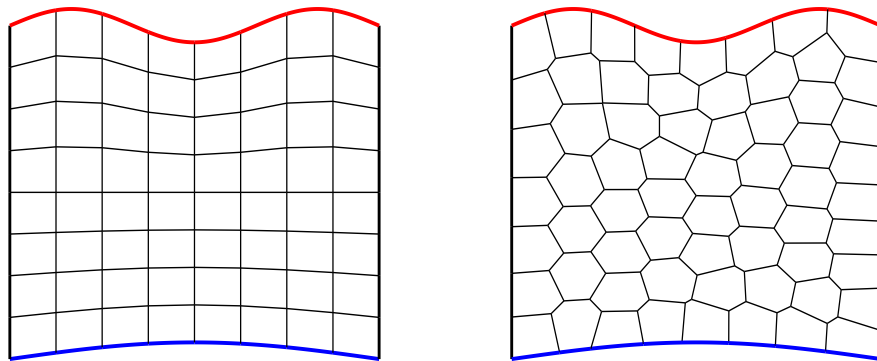
Figure 3: Example of the adopted curved polygonal meshes: quadrilateral mesh and Voronoi mesh (on the left and right), respectively.

In this experiment we test the Biharmonic problem (1.2) on the curved domain Ω. We choose the load term f and the homogeneous Dirichlet boundary conditions in such a way that the analytical solution is given by

$$u(x, y) = -(y - g_{bt}(x))^2 (y - g_{tp}(x))^2 x^2 (1 - x)^2 (3 + \sin(5x) \sin(7y)).$$

The main objective of this test is to check the performance of the proposed VEM for curved domains, in comparison with the standard VEM in straight domains. The polygonal partition on the curved domain Ω is constructed starting from a mesh for the unitary square $\Omega_Q = (0,1)^2$ and mapping the nodes accordingly to the following rule:

$$(x_\Omega, y_\Omega) = \begin{cases} (x_s, y_s + g_{bt}(x_s)(1 - 2y_s)), & \text{if } y_s \le \frac{1}{2}, \\ (x_s, 1 - y_s + g_{tp}(x_s)(2y_s - 1)), & \text{if } y_s > \frac{1}{2}, \end{cases}$$

where (x_Q, y_Q) and (x_Ω, y_Ω) denote the mesh nodes on the square domain Ω_Q and on the curved domain Ω, respectively. The edges on the curved boundary consist of an arc of the curves Γ_{bt} and Γ_{tp} (bottom and top, respectively). In Figure 3, we depict a (curved) square mesh and a (curved) Voronoi tessellation.

In Figure 4, we show the rate of convergence with the computable errors defined in (4.1) on the given sequences of meshes with uniform mesh refinements for the polynomial degree $k = 3$. We notice that the optimal rate of convergence predicted in Theorem 3.2 is attained. Moreover, the expected optimal rate of convergence in the weaker L^2- and H^1-norms (i.e., orders $\mathcal{O}(h^4)$ and $\mathcal{O}(h^3)$, respectively) are also attained. Note that we have not proved the estimate for these cases, but the optimal rate of convergence for these weaker norms can be derived by combining the tools presented here, with a duality argument as in [25, Sections 4 and 5] (see Remark 2.4).
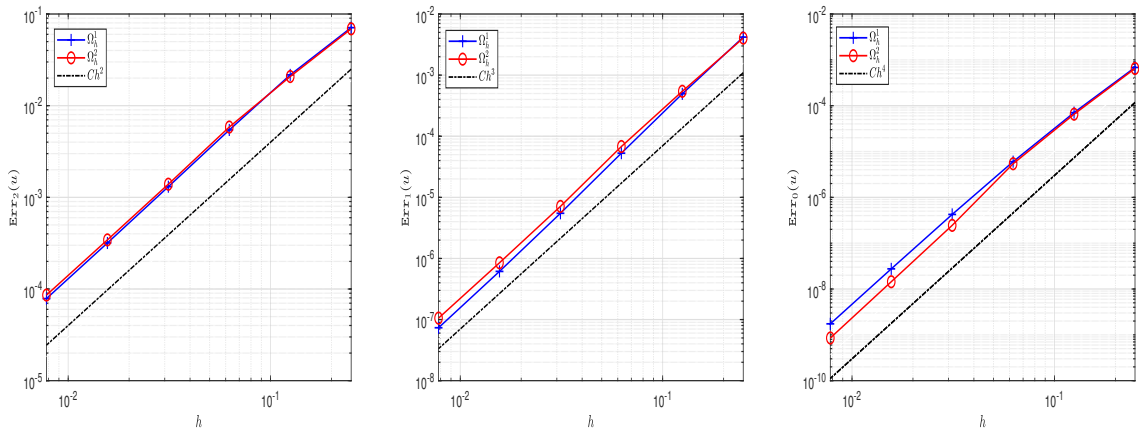

Figure 4: Errors $\text{Err}_2(u)$, $\text{Err}_1(u)$ and $\text{Err}_0(u)$ for the quadrilateral (curved) and Voronoi (curved) meshes, with $k = 3$.

As an additional test, we approximate the curved domain by employing a Voronoi tessellation sequence of elements with straight edges and we force the homogeneous Dirichlet boundary conditions; see Figure 5.
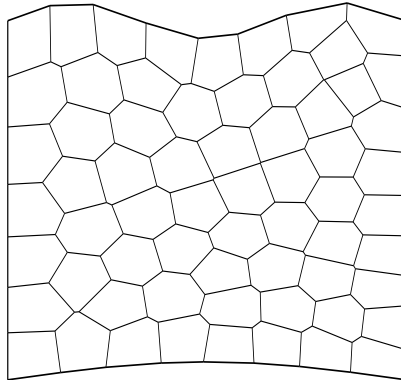

Figure 5: An example of (straight) Voronoi tessellation over the domain Ω.

In Figure 6 we show the error obtained for the sequence of Voronoi meshes on the approximated domain, by using the standard C^1-VEM on (straight) polygons.

As expected, the method obtained by the approximation of the domain with straight edge polygons suffers a loss of convergence order. We note that this loss becomes very notable for the L^2- and H^1-norms (which are only of order $\mathcal{O}(h^2)$), while for the H^2-norm can be observed a slight loss of convergence rate in the last level of refinements. In order to observe an appreciable difference also in the H^2 norm, additional experiments with $k \geq 4$ would be needed; this is beyond the current computational resources and the scopes of the present foundational contribution.
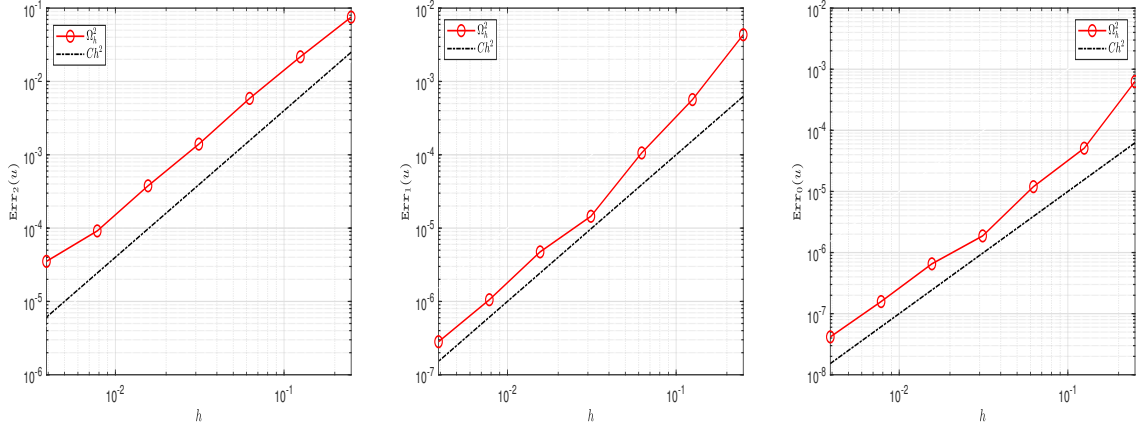
Figure 6: Errors $\mathrm{Err}_2(u)$, $\mathrm{Err}_1(u)$ and $\mathrm{Err}_0(u)$ for the quadrilateral (straight) and Voronoi (straight) meshes, with $k = 3$.

Acknowledgements

References

[1] R.A. ADAMS, AND J.J.F. FOURNIER, *Sobolev Spaces, 2nd ed.*, Academic Press, Amsterdam, 2003.

[2] B. AHMAD, A. ALSAEDI, F. BREZZI, L.D. MARINI AND A. RUSSO, *Equivalent projectors for virtual element methods*, Comput. Math. Appl., **66**, (2013), pp. 376–391.

[3] F. ALDAKHEEL, B. HUDOBIVNIK, E. ARTIOLI, L. BEIRÃO DA VEIGA AND P. WRIGGERS, *Curvilinear virtual elements for contact mechanics*, Comput. Methods Appl. Mech. Engrg., **372**, (2020), 113394, 19 pp.

[4] A. ANAND, J.S. OVALL, S.E. REYNOLDS AND S. WEISSBER, *Trefftz finite elements on curvilinear polygons*, SIAM J. Sci. Comput., **42**(2), (2020), A1289–A1316.

[5] P.F. ANTONIETTI, L. BEIRÃO DA VEIGA AND G. MANZINI, *The Virtual Element Method and Its Applications* in: SEMA SIMAI Springer Series, Springer, Cham, Vol 31, 2022.

[6] P.F. ANTONIETTI, L. BEIRÃO DA VEIGA, S. SCACCHI AND M. VERANI, *A C^1 virtual element method for the Cahn–Hilliard equation with polygonal meshes*, SIAM J. Numer. Anal., **54**, (2016), pp. 34–56.

[7] P.F. ANTONIETTI, G. MANZINI, AND M. VERANI, *The conforming virtual element method for polyharmonic problems*, Comput. Math. Appl., **79**(7), (2020), pp. 2021–2034

[8] E. ARTIOLI, L. BEIRÃO DA VEIGA AND F. DASSI, *Curvilinear virtual elements for 2D solid mechanics applications*, Comput. Methods Appl. Mech. Engrg., **359**, (2020), 112667, 19 pp.

[9] Y. BAZILEVS, L. BEIRÃO DA VEIGA, J.A. COTTRELL, T.J.R. HUGHES AND G. SANGALLI, *Isogeometric analysis: approximation, stability and error estimates for h-refined meshes*, Math. Models Methods Appl. Sci., **16**(7), (2006), pp. 1031–1090.

[10] L. BEIRÃO DA VEIGA, F. BREZZI, A. CANGIANI, G. MANZINI, L.D. MARINI AND A. RUSSO, *Basic principles of virtual element methods*, Math. Models Methods Appl. Sci., **23**, (2013), pp. 199–214.

[11] L. BEIRÃO DA VEIGA, F. BREZZI, L.D. MARINI AND A. RUSSO, *Polynomial preserving virtual elements with curved edges*, Math. Models Methods Appl. Sci., **30**(8), (2020), pp. 1555–1590.

[12] L. BEIRÃO DA VEIGA, F. BREZZI, L.D. MARINI AND A. RUSSO, *The hitchhiker's guide to the virtual element method*, Math. Models Methods Appl. Sci., **24**, (2014), pp. 1541–1573.

[13] L. BEIRÃO DA VEIGA, F. BREZZI, L.D. MARINI AND A. RUSSO, *The virtual element method*, Acta Numer., **32**, (2023), pp. 123–202.

[14] L. BEIRÃO DA VEIGA, C. LOVADINA AND A. RUSSO, *Stability analysis for the virtual element method*, Math. Models Methods Appl. Sci., **27**(13), (2017), pp. 2557–2594.

[15] L. BEIRÃO DA VEIGA, A. RUSSO AND G. VACCA, *The Virtual Element Method with curved edges*, ESAIM Math. Model. Numer. Anal., **53**(2), (2019), pp. 375–404.

[16] L. BEIRÃO DA VEIGA, Y. LIU, L. MASCOTTO AND A. RUSSO, *The nonconforming virtual element method with curved edges* J. Sci. Comput., **99**(1), (2024), Paper No. 23, 35 pp.

[17] S. BERTOLUZZA, M. PENNACCHIO AND D. PRADA, *Weakly imposed Dirichlet boundary conditions for 2D and 3D virtual elements*, Comput. Methods Appl. Mech. Engrg., **400**, (2022), Paper No. 115454, 27 pp.

[18] L. BOTTI AND D. DI PIETRO, *Assessment of hybrid high-order methods on curved meshes and comparison with discontinuous Galerkin methods*, J. Comput. Phys., **370**, (2018), pp. 58–84.

[19] S.C. BRENNER, S. GU, T. GUDI AND L.-Y. SUNG, *A quadratic C^0 interior penalty method for linear fourth order boundary value problems with boundary conditions of the Cahn–Hilliard type*, SIAM J. Numer. Anal., **50**(4), (2012), pp. 2088–2110.

[20] S.C. BRENNER AND L.Y. SUNG, *Virtual element methods on meshes with small edges or faces*, Math. Models Methods Appl. Sci., **28**(7), (2018), pp. 1291–1336.

[21] F. BREZZI AND L.D. MARINI, *Virtual elements for plate bending problems*, Comput. Methods Appl. Mech. Engrg., **253**, (2013), pp. 455–462.

[22] E. BURMAN, M. CICUTTIN, G. DELAY AND A. ERN, *An unfitted hybrid high-order method with cell agglomeration for elliptic interface problems*, SIAM J. Sci. Comput., **43**(2), (2021), A859–A882.

[23] C. CARSTENSEN, G. MALLIK AND N. NATARAJ, *Nonconforming finite element discretization for semilinear problems with trilinear nonlinearity*, IMA J. Numer. Anal., **41**, (2021), pp. 164–205.

[24] E. CHIN, AND N. SUKUMAR, *Scaled boundary cubature scheme for numerical integration over planar regions with affine and curved boundaries*, Comput. Methods Appl. Mech. Engrg., **380**, (2021), Paper No. 113796, 40 pp.

[25] C. CHINOSI AND L.D. MARINI, *Virtual element method for fourth order problems: L^2-estimates*, Comput. Math. Appl., **72**(8), (2016), pp. 1959–1967.

[26] P.G. CIARLET, *The Finite Element Method for Elliptic Problems*, SIAM, 2002.

[27] P.G. CIARLET AND P.A. RAVIART, *Interpolation theory over curved elements, with applications to finite element methods*, Comput. Methods Appl. Mech. Engrg., **1**, (1972), pp. 217–249.

[28] J.A. COTTRELL, T.J.R. HUGHES AND Y. BAZILEVS, *Isogeometric analysis: toward integration of CAD and FEA*, Wiley, Hoboken, (2009).

[29] F. DASSI, A. FUMAGALLI, D. LOSAPIO, S. SCIALÓ, A. SCOTTI AND G. VACCA, *The mixed virtual element method on curved edges in two dimensions*, Comput. Methods Appl. Mech. Engrg., **386**, (2021), Paper No. 114098, 25 pp.

[30] F. DASSI, A. FUMAGALLI, I. MAZZIERI, A. SCOTTI AND G. VACCA, *A virtual element method for the wave equation on curved edges in two dimensions*, J. Sci. Comput., **90**(1), (2022), Paper No. 50, 25 pp.

[31] F. DASSI, A. FUMAGALLI, A. SCOTTI AND G. VACCA, *Bend 3D mixed virtual element method for Darcy problems*, Comput. Math. Appl., **119**, (2022), pp. 1–12.

[32] Z. DONG AND A. ERN, *Hybrid high-order method for singularly perturbed fourth-order problems on curved domains*, ESAIM Math. Model. Numer. Anal., **55**(6), (2021), pp 3091–3114.

[33] E.H. GEORGOULIS AND P. HOUSTON, *Discontinuous Galerkin methods for the biharmonic problem*, IMA J. Numer. Anal., **29**(3), (2009), pp. 573–594.

[34] V. GIRAULT AND P.A. RAVIART, *Finite Element Methods for Navier-Stokes Equations*, Springer-Verlag, Berlin, 1986.

[35] Q. GUAN, *Some estimates of virtual element methods for fourth order problems*, Electronic Research Archive, **29**(6), (2021), pp. 4099–4118.

[36] M. FRITTELLI AND I. SGURA, *Virtual element method for the Laplace-Beltrami equation on surfaces*, ESAIM Math. Model. Numer. Anal., **52**(3), (2018), pp. 965–993.

[37] C. GÜRKAN, E. SALA-LARDIES, M. KRONBICHLER AND S. FERNÁNDEZ-MÉNDEZ, *EXtended Hybridizable Discontinous Galerkin (X-HDG) for void problems*, J. Sci. Comput., **66**(3), (2016), pp. 1313–1333.

[38] T.J.R. HUGHES, J.A. COTTRELL AND Y. BAZILEVS, *Isogeometric analysis: CAD, finite elements, NURBS, exact geometry and mesh refinement*, Comput. Methods Appl. Mech. Engrg., **194**(39-41), (2005), pp. 4135–4195.

[39] M. Lenoir, *Optimal isoparametric finite elements and error estimates for domains involving curved boundaries*, SIAM J. Numer. Anal., **23**, (1986), pp. 562–580.

[40] J.L. Lions and E. Magenes, *Problémes aux limites non homogénes et applications*, Travaux et Recherches Mathématiques, **17**, (1968), Dunod, Paris 1.

[41] D. Mora, G. Rivera and I. Velásquez, *A virtual element method for the vibration problem of Kirchhoff plates*, ESAIM Math. Model. Numer. Anal., **52**, (2018), pp. 1437–1456.

[42] D. Mora, C. Reales and A. Silgado, *A C^1-virtual element method of high order for the Brinkman equations in stream function formulation with pressure recovery*, IMA J. Numer. Anal., **42**(4), (2022), pp. 3632–3674.

[43] I. Mozolevski and E. Süli, *A priori error analysis for the hp-version of the discontinuous Galerkin finite element method for the biharmonic equation*, Comput. Methods Appl. Math., **3**(4), (2003), pp. 596–607.

[44] E. M. Stein, *Singular integrals and differentiability properties of functions*, volume 2. Princeton University Press, 1970.

[45] A. Sommariva and M. Vianello, *Product Gauss cubature over polygons based on Green's integration formula*, BIT **47**(2), (2007), pp. 441–453.

[46] A. Sommariva and M. Vianello, *Gauss–Green cubature and moment computation over arbitrary geometries*, J. Comput. Appl. Math., **231**(2), (2009), pp. 886–896.

[47] V. Thomée, *Polygonal domain approximation in Dirichlet's problem*, IMA J. Appl. Math., **11**(1), (1973), pp. 33–44.

[48] L. Yemm, *A new approach to handle curved meshes in the hybrid high-order method*, Found. Comput. Math., **24**(3), (2024), pp. 1049–1076.

[49] M. Zlámal, *Curved elements in the finite element method. I*, SIAM J. Numer. Anal., **10**, (1973), pp. 229–240.